Robust Aggregation for Federated Learning

Krishna Pillutla[1]   Sham M. Kakade[2]   Zaid Harchaoui[1]

[1] University of Washington   [2] Harvard University

Abstract

Federated learning is the centralized training of statistical models from decentralized data on mobile devices while preserving the privacy of each device. We present a robust aggregation approach to make federated learning robust to settings when a fraction of the devices may be sending corrupted updates to the server. The approach relies on a robust aggregation oracle based on the geometric median, which returns a robust aggregate using a constant number of iterations of a regular non-robust averaging oracle. The robust aggregation oracle is privacy-preserving, similar to the non-robust secure average oracle it builds upon. We establish its convergence for least squares estimation of additive models. We provide experimental results with linear models and deep networks for three tasks in computer vision and natural language processing. The robust aggregation approach is agnostic to the level of corruption; it outperforms the classical aggregation approach in terms of robustness when the level of corruption is high, while being competitive in the regime of low corruption. Two variants, a faster one with one-step robust aggregation and another one with on-device personalization, round off the paper.

1   Introduction

Federated learning is a key paradigm for machine learning and analytics on mobile, wearable and edge devices [46, 66] over wireless networks of 5G and beyond as well as edge networks and the internet of things. The paradigm has found widespread applications ranging from mobile apps deployed on millions of devices [6, 87], to sensitive healthcare applications [40, 73].

In federated learning, a number of devices with privacy-sensitive data collaboratively optimize a machine learning model under the orchestration of a central server, while keeping the data fully decentralized and private. Recent work has looked beyond supervised learning to domains such as data analytics but also semi-, self- and un-supervised learning, transfer learning, meta learning, and reinforcement learning [46, 58, 76, 91].

We study a question relevant in all these areas: robustness to corrupted updates. Federated learning relies on aggregation of updates contributed by participating devices, where the aggregation is privacy-preserving. Sensitivity to corrupted updates, caused either by adversaries intending to attack the system or due to failures in low-cost hardware, is a vulnerability of the usual approach. The standard arithmetic mean aggregation in federated learning is not robust to corruptions, in the sense that even a single corrupted update in a round is sufficient to degrade the global model for all devices. In one dimension, the median is an attractive aggregate for its robustness to outliers. We adopt this approach to federated learning by considering a classical multidimensional generalization of the median, known variously as the geometric or spatial or L_1 median [65].

Our robust approach preserves the privacy of the device updates by iteratively invoking the secure multi-party computation primitives used in typical non-robust federated learning [13, 17]. A device's updates are information theoretically protected in that they are computationally indistinguishable from random noise and the sensitivity of the final aggregate to the contribution of each device is bounded. Our approach is scalable, since the underlying secure aggregation algorithms are implemented in production systems across millions of mobile users across the planet [18]. The approach is communication-efficient, requiring a modest 1-3$\times$ the

1

communication cost of the non-robust setting to compute the non-linear aggregate in a privacy-preserving manner.

Contributions. The main take-away message of this work is:

Federated learning can be made robust to corrupted updates by replacing the weighted arithmetic mean aggregation with an approximate geometric median at 1-3 times the communication cost.

To this end, we make the following concrete contributions.

(a) *Robust Aggregation:* We design a novel robust aggregation oracle based on the classical geometric median. We analyze the convergence of the resulting federated learning algorithm, RFA, for least-squares estimation and show that the proposed method is robust to update corruption in up to half the devices in federated learning with bounded heterogeneity. We also describe an extension of the framework to handle arbitrary heterogeneity via personalization.

(b) *Algorithmic Implementation:* We show how to implement this robust aggregation oracle in a practical and privacy-preserving manner. This relies on an alternating minimization algorithm which empirically exhibits rapid convergence. This algorithm can be interpreted as a numerically stable version of the classical algorithm of Weiszfeld [85], thus shedding new light on it.

(c) *Numerical Simulations:* We demonstrate the effectiveness of our framework for data corruption and parameter update corruption, on federated learning tasks from computer vision and natural language processing, with linear models as well as convolutional and recurrent neural networks. In particular, our results show that the proposed RFA algorithm (i) outperforms the standard FedAvg [66], in high corruption and (ii) nearly matches the performance of the FedAvg in low corruption, both at *1-3 times the communication cost*. Moreover, the proposed algorithm is agnostic to the actual level of corruption in the problem instance.

We open source an implementation of the proposed approach in TensorFlow Federated [2]; cf. Appendix B for a template implementation. The Python code and scripts used to reproduce experimental results are publicly available online [1].

Overview. Section 2 describes related work, and Section 3 describes the problem formulation and tradeoffs of robustness. Section 4 proposes a robust aggregation oracle and presents a convergence analysis of the resulting robust federated learning algorithm. Finally, Section 5 gives comprehensive numerical simulations demonstrating the robustness of the proposed federated learning algorithm compared to standard baselines.

2   Related Work

Federated Learning was introduced in [66] as a distributed optimization approach to handle on-device machine learning, with secure multi-party averaging algorithms given in [9, 17]. Extensions were proposed in [7, 29, 33, 47, 50, 57, 69, 75, 79]; see also the recent surveys [46, 56]. We address robustness to corrupted updates, which is broadly applicable in these settings.

Distributed optimization has a long history [15]. Recent work includes primal-dual frameworks [62, 80] and variants suited to decentralized [37], and asynchronous [52] settings. From the lens of *learning in networks* [77], federated learning comprises a star network where agents (i.e., devices) with private data are connected to a server with no data, which orchestrates the cooperative learning. Further, for privacy, model updates from individual agents cannot be shared directly, but must be aggregated securely.

Robust estimation was pioneered by Huber [41, 42]. Robust median-of-means were introduced in [70], with follow ups in [39, 53, 60, 61, 67]. Robust mean estimation, in particular, received much attention [25,

28, 68]. Robust estimation in networks was considered in [4, 24, 89]. These works consider the statistics of robust estimation in the i.i.d. case, while we focus on distributed optimization with privacy preservation.

Byzantine robustness, resilience to arbitrary behavior of some devices [51], was studied in distributed optimization with gradient aggregation [5, 16, 20, 21, 23, 88]. Byzantine robustness of federated learning is a priori not possible without additional assumptions because the secure multi-party computation protocols require faithful participation of the devices. Thus, we consider a more nuanced and less adversarial corruption model where devices participate faithfully in the aggregation loop; see Section 3 for practical examples. Further, it is unclear how to securely implement the nonlinear aggregation algorithms of these works. Lastly, the use of, e.g., secure enclaves [81] in conjunction with our approach could guarantee Byzantine robustness in federated learning. We aggregate *model parameters* in a robust manner, which is more suited to the federated setting. We note that [55] also aggregate model parameters rather than gradients by framing the problem in terms of consensus optimization. However, their algorithm requires devices to be always available and participate in multiple rounds, which is not practical in the federated setting [46].

Weiszfeld's algorithm [85] to *compute the geometric median*, has received much attention [11, 49, 83]. The Weiszfeld algorithm is also known to exhibit asymptotic linear convergence [48]. However, unlike these variants, ours is numerically stable. A theoretical proposal of a near-linear time algorithm for the geometric median was recently explored in [27].

Frameworks to guarantee *privacy* of user data include differential privacy [31, 45] and homomorphic encryption [35]. These directions are orthogonal to ours, and could be used in conjunction. See [17, 46, 56] for a broader discussion.

3 Problem Setup: Federated Learning with Corruptions

We begin this section by recalling the setup of federated learning (without corruption) and the standard FedAvg algorithm [66] in Section 3.1. We then formally setup our corruption model and discuss the trade-offs introduced by requiring robustness to corrupted updates in Section 3.2.

3.1 Federated Learning Setup and Review

Federated learning consists of n client devices which collaboratively train a machine learning model under the orchestration of a central server or a fusion center [46, 66]. The data is local to the client devices while the job of the server is to orchestrate the training.

We consider a typical federated learning setting where each device i has a distribution D_i over some data space such that the data on the client is sampled i.i.d. from D_i. Let the vector $w \in \mathbb{R}^d$ denote the parameters of a (supervised) learning model and let $f(w; z)$ denote the loss of model w on input-output pair z, such as the mean-squared-error loss. Then, the objective function of device i is $F_i(w) = \mathbb{E}_{z \sim D_i}[f(w; z)]$.

Federated learning aims to find a model $w^\star$ that minimizes the average objective across all the devices,

$$\min_{w \in \mathbb{R}^d} \left[F(w) := \sum_{i=1}^n \alpha_i \, F_i(w) \right], \tag{1}$$

where device i is weighted by $\alpha_i > 0$. In practice, the weight α_i is chosen proportional to the amount of data on device i. For instance, in an empirical risk minimization setting, each D_i is the uniform distribution over a finite set $\{z_{i,1}, \cdots, z_{i,N_i}\}$ of size N_i. It is common practice to choose $\alpha_i = N_i/N$ where $N = \sum_{i=1}^n N_i$ so that the objective $F(w) = (1/N) \sum_{i=1}^n \sum_{j=1}^{N_i} f(w; z_{i,j})$ is simply the unweighted average over all samples from all n devices.

Federated Learning Algorithms. Typical federated learning algorithms run in synchronized rounds of communication between the server and the devices with some local computation on the devices based on their local data, and aggregation of these updates to update the server model. The de facto standard training algorithm is FedAvg [66], which runs as follows.

(a) The server samples a set S_t of m clients from $[n]$ and broadcasts the current model $w^{(t)}$ to these clients.

(b) Staring from $w_{i,0}^{(t)} = w^{(t)}$, each client $i \in S_t$ makes τ local gradient or stochastic gradient descent steps for $k = 0, \cdots, \tau - 1$ with a learning rate γ:

$$w_{i,k+1}^{(t)} = w_{i,k}^{(t)} - \gamma \nabla F_i(w_{i,k}^{(t)}). \tag{2}$$

(c) Each device $i \in S_t$ sends to the server a vector $w_i^{(t+1)}$ which is simply the final iterate, i.e., $w_i^{(t+1)} = w_{i,\tau}^{(t)}$. The server updates its global model using the weighted average

$$w^{(t+1)} = \frac{\sum_{i \in S_t} \alpha_i w_i^{(t+1)}}{\sum_{i \in S_t} \alpha_i}. \tag{3}$$

The federated learning algorithm, and in particular, the choice of aggregation, impacts the following three factors [34, 46, 56]: communication efficiency, privacy, and robustness.

Communication Efficiency. Besides the computation cost, the communication cost is an important parameter in distributed optimization. While communication is relatively fast in the datacenter, that is not the case of federated learning. The repeated exchange of massive models between the server and client devices over resource-limited wireless networks makes communication over the network more of a bottleneck in federated learning than local computation on the devices. Therefore, training algorithms should be able to trade-off more local computation for lower communication, similar to step (b) of FedAvg above. While the exact benefits (or lack thereof) of local steps is an active area of research, local steps have been found empirically to reduce the amount of communication required for a moderately accurate solution [66, 84].

Accordingly, we set aside the local computation cost for a first order approximation, and compare algorithms in terms of their total communication cost [46]. Since typical federated learning algorithms proceed in synchronized rounds of communication, we measure the complexity of the algorithms in terms of the number of communication rounds.

Privacy. While the privacy-sensitive data $z \sim D_i$ is kept local to the device, the model updates $w_i^{(t+1)}$ might also leak privacy. To add a further layer of privacy protection, the server is not allowed to inspect individual updates $w_i^{(t+1)}$ in the aggregation step (c); it can only access the aggregate $w^{(t+1)}$.

We make this precise through the notion of a *secure average oracle*. Given m devices with each device i containing $w_i \in \mathbb{R}^d$ and a scalar $\beta_i > 0$, a secure average oracle computes the average $\sum_{i=1}^m \beta_i w_i / \sum_{i=1}^m \beta_i$ at a total communication of $\mathcal{O}(md + m \log m)$ bits such that no w_i or β_i are revealed to either the server or any other device.

In practice, a secure average oracle is implemented using cryptographic protocols based on secure multi-party computation [13, 17]. These require a communication overhead of $O(m \log m)$ in addition to $O(md)$ cost of sending the m vectors. First, the vector $\beta_i w_i$ is dimension-wise discretized on the ring $\mathbb{Z}_M^d$ of integers modulo M in d-dimensions. Then, a noisy version $\tilde{w}_i$ is sent to the server, where the noise is designed to satisfy:

- correctness up to discretization, by ensuring $\sum_{i=1}^m \tilde{w}_i \mod M = \sum_{i=1}^m \beta_i w_i \mod M$ with probability 1, and,
- privacy preservation from honest-but-curious devices and server in the information theoretic sense, by ensuring that $\tilde{w}_i$ is computationally indistinguishable from $\zeta_i \sim \text{Uniform}(\mathbb{Z}_M^d)$, irrespective of w_i and β_i.

Table 1: Examples corruptions and capability of an adversary they require, as measured along the following axes: **Data write**, where a device $i \in \mathcal{C}$ can replace its local distribution D_i by any arbitrary distribution $\tilde{D}_i$; **Model read**, where a device $i \in \mathcal{C}$ can read the server model $w^{(t)}$ and replace its local distribution D_i by an adaptive distribution $\tilde{D}_i^{(t)}$ depending on $w^{(t)}$; **Model write**, where a device $i \in \mathcal{C}$ can return an arbitrary vector to the server for aggregation as in (4), and, **Aggregation**, where a device $i \in \mathcal{C}$ can behave arbitrarily during the computation of an iterative secure aggregate. The last column indicates whether the proposed RFA algorithm is robust to each type of corruption.

Corruption Type	Data write	Model read	Model write	Aggregation	RFA applicable?
Non-adversarial	-	-	-	-	✓
Static data poisoning	Yes	-	-	-	✓
Adaptive data poisoning	Yes	Yes	-	-	✓
Update poisoning	Yes	Yes	Yes	-	✓
Byzantine	Yes	Yes	Yes	Yes	N/A

As a result, we get the correct average (up to discretization) while not revealing any further information about a w_i or β_i to the server or other devices, beyond what can be inferred from the average. Hence, no further information about the underlying data distribution D_i is revealed either. In this work, we assume for simplicity that the secure average oracle returns the exact update, i.e., we ignore the effects of discretization on the integer ring and modular wraparound. This assumption is reasonable for a large enough value of M.

Robustness. We would like a federated learning algorithm to be robust to corrupted updates contributed by malicious devices or hardware/software failures. FedAvg uses an arithmetic mean to aggregate the device updates in (3), which is known to not be robust [41]. This can be made precise by the notion of a breakdown point [30], which is the smallest fraction of the points which need to be changed to cause the aggregate to take on arbitrary values. The breakdown point of the mean is 0, since only one point needs to changed to arbitrarily change the aggregate [65]. This means in federated learning that a single corrupted update, either due to an adversarial attack or a failure, can arbitrarily change the resulting aggregate in each round. We will give examples of adversarial corruptions in Section 3.2.

In the rest of this work, we aim to address the lack of robustness of FedAvg. A popular robust aggregation of scalars is the median rather than the mean. We investigate a multidimensional analogue of the median, while respecting the other two factors: communication efficiency and privacy. While the non-robust mean aggregation can be computed with secure multi-party computation via the secure average oracle, it is unclear if a robust aggregate can also satisfy this requirement. We discuss this as well as other tradeoffs involving robustness in the next section.

3.2 Corruption Model and Trade-offs of Robustness

We start with the corruption model used in this work. We allow a subset $\mathcal{C} \subset [n]$ of *corrupted devices* to, unbeknownst to the server, send arbitrary vectors $w_i^{(t+1)} \in \mathbb{R}^d$ rather than the updated model $w_{i,\tau}^{(t)}$ from local data as expected by the server. Formally, we have,

$$w_i^{(t+1)} = \begin{cases} w_{i,\tau}^{(t)}, & \text{if } i \notin \mathcal{C}, \\ H_i\left(w^{(t)}, \{(w_{j,\tau}^{(t)}, D_j)\}_{j \in S_t}\right) & \text{if } i \in \mathcal{C}, \end{cases} \tag{4}$$

where H_i is an arbitrary $\mathbb{R}^d$-valued function which is allowed to depend on the global model $w^{(t)}$, the uncorrupted updates $w_{j,\tau}^{(t)}$ as well as the data distributions D_j of each device $j \in S_t$.

This encompasses situations where the corrupted devices are individually or collectively trying to "attack" the global model, that is, reduce its predictive power over uncorrupted data. We define the *corruption level* ρ as the total fraction of the weight of the corrupted devices:

$$\rho = \frac{\sum_{i \in \mathcal{C}} \alpha_i}{\sum_{i=1}^{n} \alpha_i}. \tag{5}$$

Since the corrupted devices can only harm the global model through the updates they contribute in the aggregation step, we aim to robustify the aggregation in federated learning. However, it turns out that robustness is not directly compatible with the two other desiderata of federated learning, namely communication efficiency and privacy.

The Tension Between Robustness, Communication and Privacy. We first argue that any federated learning algorithm can only have two out of the three of robustness, communication and privacy under the existing techniques of secure multi-party computation. The standard approach of FedAvg is communication-efficient and privacy-preserving but not robust, as we discussed earlier. In fact, any aggregation scheme $A(w_1, \cdots, w_m)$ which is a linear function of $w_1, \cdots, w_m$ is similarly non-robust. Therefore, any robust aggregate A must be a non-linear function of the vectors it aggregates.

The approach of sending the updates to the server at a communication of $O(md)$ and utilizing one of the many robust aggregates studied in the literature [e.g. 5, 23, 88] has robustness and communication efficiency but not privacy. If we try to make it privacy-preserving, however, we lose communication efficiency. Indeed, the secure multi-party computation primitives based on secret sharing, upon which privacy-preservation is built, are communication efficient only for linear functions of the inputs [32]. The additional $O(m \log m)$ overhead of secure averaging for linear functions becomes $\Omega(md \log m)$ for general non-linear functions required for robustness; this makes it impractical for large-scale systems [17]. Therefore, one cannot have both communication efficiency and privacy preservation along with robustness.

In this work, we strike a compromise between robustness, communication and privacy. We will approximate a non-linear robust aggregate as an *iterative secure aggregate*, i.e., as a sequence of weighted averages, computed with a secure average oracle with weights being adaptively updated.

Definition 1. *A function $A : (\mathbb{R}^d)^m \to \mathbb{R}^d$ is said to be an iterative secure aggregate of $w_1, \cdots, w_m$ with R communication rounds and initial iterate $v^{(0)}$ if for $r = 0, \cdots, R - 1$, there exist weights $\beta_1^{(r)}, \cdots, \beta_m^{(r)}$ such that*
(i) $\beta_i^{(r)}$ depends only on $v^{(r)}$ and w_i,
(ii) $v^{(r+1)} = \sum_{i=1}^{m} \beta_i^{(r)} w_i / \sum_{i=1}^{m} \beta_i^{(r)}$, and,
(iii) $A(w_1, \cdots w_m) = v^{(R)}$.
Further, the iterative secure aggregate is said to be s-privacy preserving for some $s \in (0, 1)$ if
(iv) $\beta_i^{(r)} / \sum_{j=1}^{m} \beta_j^{(r)} \leq s$ for all $i \in [m]$ and $r \in [R]$.

If we have an iterative secure aggregate with R communication rounds which is also robust, we gain robustness at a R-fold increase in communication cost. Condition (iv) ensures privacy preservation because it reveals only weighted averages with weights at most s, so a user's update is only available after being mixed with those from a large cohort of devices.

The Tension Between Robustness and Heterogeneity. Heterogeneity is a key property of federated learning. The distribution D_i of device i can be quite different from the distribution D_j of some other device j, reflecting the heterogeneous data generated by a diverse set of users.

To analyze the effect of heterogeneity on robustness, consider the simplified scenario of robust mean estimation in Huber's contamination model [41]. Here, we wish to estimate the mean $\mu \in \mathbb{R}^d$ given

samples $w_1, \cdots, w_m \sim (1-\rho)\mathcal{N}(\mu, \sigma^2 I) + \rho Q$, where Q denotes some outlier distribution that ρ-fraction of the points (designated as outliers) are drawn from. Any aggregate $\bar{w}$ must satisfy the lower bound $\|\bar{w} - \mu\|^2 \geq \Omega(\sigma^2 \max\{\rho^2, d/m\})$ with constant probability [22, Theorem 2.2]. In the federated learning setting, more heterogeneity corresponds to a greater variance σ^2 among the inlier points, implying a larger error in mean estimation. This suggests a tension between robustness and heterogeneity, where increasing heterogeneity makes robust mean estimation harder in terms of ℓ_2 error.

In this work, we strike a compromise between robustness and heterogeneity by considering a family $\mathcal{D}$ of allowed data distributions such that any device i with $D_i \notin \mathcal{D}$ will be regarded as a corrupted device, i.e., $i \in \mathcal{C}$. We will be able to guarantee convergence up to the degree of heterogeneity in $\mathcal{D}$; we call this $\mathrm{width}(\mathcal{D})$ and make it precise in Section 4. In the i.i.d. case, $\mathcal{D}$ is a singleton and $\mathrm{width}(\mathcal{D}) = 0$.

Examples. Next, we consider some examples of update corruption — see [46] for a comprehensive treatment. Corrupted updates could be non-adversarial in nature, such as sensor malfunctions or hardware bugs in unreliable and heterogeneous devices (e.g., mobile phones) which are outside the control of the orchestrating server. On the other hand, we could also have adversarial corruptions of the following types:

(a) *Static data poisoning:* The corrupted devices $\mathcal{C}$ are allowed to modify their training data prior to the start of the training, and the data is fixed thereafter. Formally, the objective function of device $i \in \mathcal{C}$ is now $\tilde{F}_i(w) = \mathbb{E}_{z \sim \tilde{D}_i}[f(w; z)]$ where $\tilde{D}_i$ has been modified from the original D_i. These devices then participate in the local updates (2) with $\nabla \tilde{F}_i$ rather than ∇F_i. We consider device i to contribute corrupted updates only if $\tilde{D}_i \notin \mathcal{D}$ (for instance, $\mathcal{D}$ is the set of natural RGB images).

(b) *Adaptive data poisoning:* The corrupted devices $\mathcal{C}$ are allowed to modify their training data in each round of training depending on the current model $w^{(t)}$. Concretely, the objective function of device $i \in \mathcal{C}$ in round t is $\tilde{F}_i^{(t)}(w) = \mathbb{E}_{z \sim \tilde{D}_i^{(t)}}[f(w; z)]$ where $\tilde{D}_i^{(t)}$ has been modified from the original D_i using knowledge of $w^{(t)}$. As previously, these devices then participate in the local updates (2) with $\nabla \tilde{F}_i^{(t)}$ rather than ∇F_i in round t.

(c) *Update Poisoning:* The corrupted devices can send an arbitrary vector to the server for aggregation, as described by (4) in its full generality. This setting subsumes all previous examples as special cases.

The corruption model in (4) precludes the *Byzantine setting* [e.g., 46, Sec. 5.1], which refers to the worst-case model where a corrupted client device $i \in \mathcal{C}$ can behave arbitrarily, such as for instance, changing the weights $\beta_i^{(r)}$ or the vector w_i between each of the rounds of the iterative secure aggregate, as defined in Definition 1. It is provably impossible to design a Byzantine-robust iterative secure aggregate in this sense. The examples listed above highlight the importance of robustness to the corruption model under consideration.

Table 1 compares the various corruptions in terms of the capability of an adversary required to induce the corruption.

4 Robust Aggregation and the RFA Algorithm

In this section, we design a robust aggregation oracle and analyze the convergence of the resulting federated algorithm.

Robust Aggregation with the Geometric Median. The geometric median (GM) of $w_1, \cdots, w_m \in \mathbb{R}^d$ with weights $\alpha_1, \cdots, \alpha_m > 0$ is the minimizer of

$$g(v) := \sum_{i=1}^{m} \alpha_i \|v - w_i\|, \tag{6}$$

Algorithm 1 The RFA Algorithm

Input: Initial iterate $w^{(0)}$, number of communication rounds T, number of clients per round m, number of
local updates τ, local step size γ, approximation threshold ϵ

1: **for** $t = 0, 1, \cdots, T - 1$ **do**
2:      Sample m clients from $[n]$ without replacement in S_t
3:      **for** each selected client $i \in S_t$ in parallel **do**
4:          Initialize $w_{i,0}^{(t)} = w^{(t)}$
5:          **for** $k = 0, \cdots, \tau - 1$ **do**
6:              Sample data $z_{i,k}^{(t)} \sim D_i$
7:              Update $w_{i,k+1}^{(t)} = w_{i,k}^{(t)} - \gamma \nabla f(w_{i,k}^{(t)}; z_{i,k}^{(t)})$
8:          Set $w_i^{(t+1)} = w_{i,\tau}^{(t)}$
9:      $w^{(t+1)} = \mathrm{GM}\big((w_i^{(t+1)})_{i \in S_t}, (\alpha_i)_{i \in S_t}, \epsilon\big)$ (Algo. 2)
10: **return** w_T

---

where $\|\cdot\| = \|\cdot\|_2$ is the Euclidean norm. As a robust aggregation oracle, we use an ϵ-approximate minimizer $\widehat{v}$ of g which satisfies $g(\widehat{v}) - \min_z g(v) \leq \epsilon$. We denoted it by $\widehat{v} = \mathrm{GM}\left((w_i)_{i=1}^m, (\alpha_i)_{i=1}^m, \epsilon\right)$. Further, when $\alpha_i = 1/m$, we write $\mathrm{GM}\left((w_i)_{i=1}^m, \epsilon\right)$.

The GM has an optimal breakdown point of 1/2 [59]. That is, to get the geometric median to equal an arbitrary point, at least half the points (in total weight) must be modified. We assume that $w_1, \cdots w_m$ are non-collinear, which is reasonable in the federated setting. Then, g admits a unique minimizer $v^\star$. Further, we assume $\sum_i \alpha_i = 1$ w.l.o.g.[1]

Robust Federated Aggregation: The RFA Algorithm. The RFA algorithm is obtained by replacing the mean aggregation of FedAvg with this GM-based robust aggregation oracle – the full algorithm is given in Algorithm 1. Similar to FedAvg, RFA also trades-off some communication for local computation by running multiple local steps in line 5. The communication efficiency and privacy preservation of RFA follow from computing the GM as an iterative secure aggregate, which we turn to next. Note that RFA is agnostic to the *actual* level of corruption in the problem and the aggregation is robust regardless of the convexity of the local objectives F_i.

Geometric Median as an Iterative Secure Aggregate. While the GM is a natural robust aggregation oracle, the key challenge in the federated setting is to implement it as an iterative secure aggregate. Our approach, given in Algorithm 2, iteratively computes a new weight $\beta_i^{(r)} \propto 1/\|v^{(r)} - w_i\|$, up to a tolerance $\nu > 0$, whose role is to prevent division by zero. This endows the algorithm with greater stability. We call it the smoothed Weiszfeld algorithm as it is a variation of Weiszfeld's classical algorithm [85]. The smoothed Weiszfeld algorithm satisfies the following convergence guarantee, proved in Appendix C.

Proposition 2. *The iterate $v^{(R)}$ of Algorithm 2 with input $v^{(0)} \in \mathrm{conv}\{w_1, \cdots, w_m\}$ and $\nu > 0$ satisfies*

$$g(v^{(R)}) - g(v^\star) \leq \frac{2\|v^{(0)} - v^\star\|^2}{\overline{\nu} R} + \frac{\nu}{2},$$

where $v^\star = \arg\min g$ and $\overline{\nu} = \min_{r \in [R], i \in [m]} \nu \vee \|v^{(r-1)} - w_i\| \geq \nu$. Furthermore, if $0 < \nu \leq \min_{i=1,\cdots,m} \|v^\star - w_i\|$, then it holds that $g(v^{(R)}) - g(v^\star) \leq 2\|v^{(0)} - v^\star\|^2/\overline{\nu} R$.

---

[1] One could apply the results to $\widetilde{g}(v) := g(v)/\sum_{i=1}^m \alpha_i$.

Algorithm 2 The Smoothed Weiszfeld Algorithm

Input: $w_1, \cdots, w_m \in \mathbb{R}^d$ with w_i on device i, $\alpha_1, \cdots, \alpha_m > 0$, $\nu > 0$, budget R, $v^{(0)} \in \mathbb{R}^d$, secure average oracle $\mathcal{A}$

1: **for** $r = 0, 1, \cdots, R - 1$ **do**
2:      Server broadcasts $v^{(r)}$ to devices $1, \cdots, m$
3:      Device i computes $\beta_i^{(r)} = \alpha_i / (\nu \vee \|v^{(r)} - w_i\|)$
4:      $v^{(r+1)} \leftarrow \left(\sum_{i=1}^m \beta_i^{(r)} w_i \right) / \sum_{i=1}^m \beta_i^{(r)}$ using $\mathcal{A}$
    return $v^{(R)}$

For a ϵ-approximate GM, we set $\nu = O(\epsilon)$ to get a $O(1/\epsilon^2)$ rate. However, if the GM $v^\star$ is not too close to any w_i, then the same algorithm automatically enjoys a faster $O(1/\epsilon)$ rate. The algorithm enjoys plausibly an even faster convergence rate *locally*, and we leave this for future work.

The proof relies on constructing a jointly convex surrogate $G : \mathbb{R}^d \times \mathbb{R}_{++}^m \to \mathbb{R}$ defined using $\eta = (\eta_1, \cdots, \eta_m) \in \mathbb{R}^m$ as

$$G(v, \eta) := \frac{1}{2} \sum_{k=1}^m \alpha_k \left(\frac{\|v - w_k\|^2}{\eta_k} + \eta_k \right).$$

Instead of minimizing $g(v)$ directly using the equality $g(v) = \inf_{\eta > 0} G(v, \eta)$, we impose the constraint $\eta_i \geq \nu$ instead to avoid division by small numbers. The following alternating minimization leads to Algorithm 2:

$$\eta^{(r)} = \underset{\eta \geq \nu}{\arg\min}\, G(v^{(r)}, \eta), \text{ and, } v^{(r+1)} = \underset{v \in \mathbb{R}^d}{\arg\min}\, G(v, \eta^{(r)}).$$

Numerically, we find in Figure 1 that Algorithm 2 is rapidly convergent, giving a **high quality solution in 3 iterations**. This ensures that the approximate GM as an iterative secure aggregate provides robustness at a modest $3\times$ increase in communication cost over regular mean aggregation in FedAvg.

Privacy Preservation. While we can compute the geometric median as an iterate secure aggregate, privacy preservation also requires that the effective weights $\beta_i^{(r)} / \sum_j \beta_j^{(r)}$ are bounded away from 1 for each i. We show this holds for m large.

Proposition 3. *Consider $\beta^{(r)}, v^{(r)}$ produced by Algorithm 2 when given $w_1, \cdots w_m \in \mathbb{R}^d$ with weights $\alpha_i = 1/m$ for each i as inputs. Denote $B = \max_{i,j} \|w_i - w_j\|$ and $\bar{\nu}$ as in Proposition 2. Then, we have for all $i \in [m]$ and $r \in [R]$ that*

$$\frac{\beta_i^{(r)}}{\sum_{j=1}^m \beta_j^{(r)}} \leq \frac{B}{B + (m-1)\bar{\nu}}.$$

Proof. Since $v^{(r)} \in \mathrm{conv}\{w_1, \cdots, w_m\}$, we have $\bar{\nu} \leq \|v^{(r)} - w_i\| \leq B$. Hence, $\alpha_i/B \leq \beta_i^{(r)} \leq \alpha_i/\bar{\nu}$ for each i and r and the proof follows. $\qquad\square$

4.1 Convergence Analysis of RFA

We now present a convergence analysis of RFA under two simplifying assumptions. First, we focus on least-squares fitting of additive models, as it allows us to leverage sharp analyses of SGD [8, 43, 44] and focus on the effect of the aggregation. Second, we assume w.l.o.g. that each device is weighted by $\alpha_i = 1/n$ to avoid technicalities of random sums $\sum_{i \in S_t} \alpha_i$. This assumption can be lifted with standard reductions; see Remark 5.
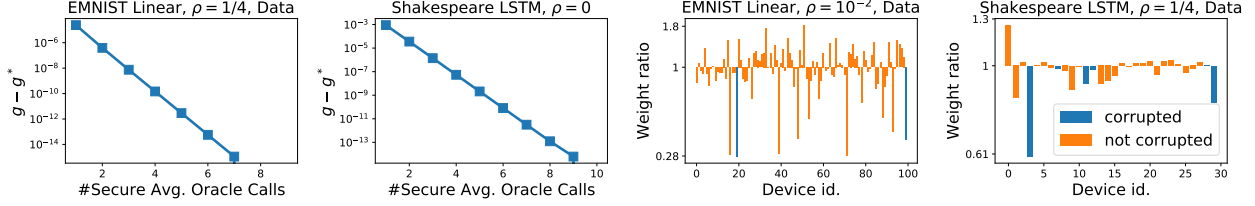
Figure 1: **Left two**: Convergence of the smoothed Weiszfeld algorithm. **Right two**: Visualization of the re-weighting β_i/α_i, where β_i is the weight of w_i in $\mathrm{GM}((w_i),(\alpha_i)) = \sum_i \beta_i w_i$. See Appendix D.4 for details.

Setup. We are interested in the supervised learning setting where $z_i \equiv (x_i, y_i) \sim D_i$ is an input-output pair. We assume that the output y_i satisfies $\mathbb{E}[y_i] = 0$ and $\mathbb{E}[y_i^2] < \infty$. Denote the marginal distribution of input x_i as $D_{X,i}$. The goal is to estimate the regression function $\overline{x} \mapsto \mathbb{E}[y_i|x_i = \overline{x}]$ from a training sequence of independent copies of $(x_i, y_i) \sim D_i$ in each device. The corresponding objective is the square loss minimization

$$F(w) = \frac{1}{n} \sum_{i=1}^n F_i(w), \quad \text{where} \quad F_i(w) = \frac{1}{2} \mathbb{E}_{(x,y)\sim D_i} \left(y - w^\top \phi(x) \right)^2 \quad \text{for all } i \in [n]. \tag{7}$$

Here, $\phi(x) = (\phi_1(x), \ldots, \phi_d(x)) \in \mathbb{R}^d$ where $\phi_1, \ldots, \phi_d$ are a fixed basis of measurable, centered functions. The basis functions may be nonlinear, thus encompassing random feature approximations of kernel feature maps and pre-trained deep network feature representations.

We state our results under the following assumptions: (a) the feature maps are bounded as $\|\phi(x)\| \leq R$ with probability one under $D_{X,i}$ for each device i; (b) each F_i is μ-strongly convex; (c) the additive model is well-specified on each device: for each device i, there exists $w_i^\star \in \mathbb{R}^d$ such that $y_i = \phi(x_i)^\top w_i^\star + \zeta_i$ where $\zeta_i \sim \mathcal{N}(0, \sigma^2)$. The second assumption is equivalent to requiring that $H_i = \nabla^2 F_i(w) = \mathbb{E}_{x\sim D_{X,i}}[\phi(x)\phi(x)^\top]$, the covariance of x on device i has eigenvalues no smaller than μ.

Quantifying Heterogeneity. We quantify the heterogeneity in the data distributions D_i across devices in terms of the heterogeneity of marginals $D_{X,i}$ and of the conditional expectation $\mathbb{E}[y_i|x_i = x] = \phi(x)^\top w_i^\star$. Let $H = \nabla^2 F(w) = (1/n) \sum_{i=1}^n H_i$ be the covariance of x under the mixture distribution across devices, where H_i is the covariance of x_i in device i. We measure the dissimilarities $\Omega_X, \Omega_{Y|X}$ of the marginal and the conditionals respectively as

$$\Omega_X = \max_{i\in[n]} \lambda_{\max}(H^{-1/2}H_i H^{-1/2}), \quad \text{and,} \quad \Omega_{Y|X} = \max_{i,j\in[n]} \|w_i^\star - w_j^\star\|, \tag{8}$$

where $\lambda_{\max}(\cdot)$ denotes the largest eigenvalue. Note that $\Omega_X \geq 1$ and it is equal to 1 iff each $H_i = H$. It measures the spectral misalignment between each H_i and H. The second condition is related to the Wasserstein-2 distance [72] between the conditionals $D_{Y|X,i}$ as $W_2(D_{Y|X,i}, D_{Y|X,j}) \leq R\Omega_{Y|X}$. We define the degree of heterogeneity between the various $D_i = D_{X,i} \otimes D_{Y|X,i}$ as $\mathrm{width}(\mathcal{D}) = \Omega_X \Omega_{Y|X} =: \Omega$. That is, if the conditionals are the same ($\Omega_{Y|X} = 0$), we can tolerate arbitrary heterogeneity in the marginals $D_{X,i}$.

Convergence. We now analyze RFA where the local SGD updates are equipped with "tail-averaging" [44] so that $w_i^{(t+1)} = (2/\tau) \sum_{k=\tau/2}^\tau w_{i,k}^{(t)}$ is averaged over the latter half of the trajectory of iterates instead of line 8 of Algorithm 1. We show that this variant of RFA converges up to the dissimilarity level $\Omega = \Omega_X \Omega_{Y|X}$ when the corruption level $\rho < 1/2$.

Theorem 4. *Consider F defined in (7) and suppose the corruption level satisfies $\rho < 1/2$. Consider Algorithm 1 run for T outer iterations with a learning rate $\gamma = 1/(2R^2)$, and the local updates are run for τ_t steps in outer iteration t with tail averaging. Fix $\delta > 0$ and $\theta \in (\rho, 1/2)$, and set the number of devices per iteration, m as*

$$m \geq \frac{\log(T/\delta)}{2(\theta - \rho)^2} \, . \tag{9}$$

Define $C_\theta := (1 - 2\theta)^{-2}$, $w^\star = \arg\min F$, $F^\star = F(w^*)$, $\kappa := R^2/\mu$ and $\Delta_0 := \|w^{(0)} - w^\star\|^2$. Let $\tau \geq 4\kappa \log(128 C_\theta \kappa)$. We have that the event $\mathcal{E} = \bigcap_{t=0}^{T-1}\{|S_t \cap \mathcal{C}| \leq \theta m\}$ holds with probability at least $1 - \delta$. Further, if $\tau_t = 2^t \tau$ for each iteration t, then the output $w^{(T)}$ of Algorithm 1 satisfies,

$$\mathbb{E}\left[\|w^{(T)}) - w^\star\|^2 \,\Big|\, \mathcal{E}\right] \leq \frac{\Delta_0}{2^T} + CC_\theta \left(\frac{d\sigma^2 T}{\mu\tau 2^T} + \frac{\epsilon^2}{m^2} + \Omega^2\right)$$

where C is a universal constant. If $\tau_t = \tau$ instead, then, the noise term above reads $d\sigma^2/\mu\tau$.

Theorem 4 shows near-linear convergence $O(T/2^T)$ up to two error terms in the case that ρ is bounded away from $1/2$ (so that θ and C_θ can be taken to be constants). The increasing local computation $\tau_t = 2^t \tau$ required by this rate is feasible since local computation is assumed to be cheaper than communication.

The first error term is ϵ^2/m^2 due to approximation ϵ in the GM, which can be made arbitrarily small by increasing the number m of devices sampled per round. The second error term Ω^2 is due to heterogeneity. Indeed, exact convergence as $T \to \infty$ is not possible in the presence of corruption: lower bounds for robust mean estimation [e.g. 22, Theorem 2.2] imply that $\|w^{(T)} - w^\star\|^2 \geq C\rho^2\Omega_{Y|X}^2$ w.p. at least $1/2$. Consistent with our theory, we find in real heterogeneous datasets in Section 5 that RFA can lead to *marginally* worse performance than FedAvg in the corruption-free regime ($\rho = 0$). Finally, while we focus on the setting of least squares, our results can be extended to the general convex case.

Remark 5. *For unequal weights, we can perform the reduction $\tilde{F}_i(w) = n\alpha_i F_i(w)$, so the theory applies with the substitution $(R^2, \sigma^2, \mu, \Omega_X) \mapsto (c_1 R^2, c_1 \sigma^2, c_2 \mu, (c_1/c_2)\Omega_X)$, where $c_1 = n\max_i \alpha_i$ and $c_2 = n\min_i \alpha_i$.*

We use the following convergence result of SGD [43, Theorem 1], [44, Corollary 2].

Theorem 6 ([43, 44])**.** *Consider a F_k from (7). Then, defining $\kappa := R^2/\mu$, the output $\overline{v}_\tau$ of τ steps of tail-averaged SGD starting from $v_0 \in \mathbb{R}^d$ using learning rate $(2R^2)^{-1}$ satisfies*

$$\mathbb{E}\|\overline{v}_\tau - w^\star\|^2 \leq 2\kappa \exp\left(-\frac{\tau}{4\kappa}\right)\|v_0 - w^\star\|^2 + \frac{8d\sigma^2}{\mu\tau} \, .$$

Proof of Theorem 4. Define the event $\mathcal{E}_t = \{|S_t \cap \mathcal{C}| \leq \theta m\}$ so that $\mathcal{E} = \bigcap_{t=0}^{T-1}\mathcal{E}_t$. Hoeffding's inequality gives $\mathbb{P}(\overline{\mathcal{E}_t}) \leq \delta/T$ for each t so that $\mathbb{P}(\overline{\mathcal{E}}) \leq \delta$ using the union bound. Below, let $\mathcal{F}_t$ denote the sigma algebra generated by $w^{(t)}$.

Consider the local updates on an uncorrupted device $i \in S_t \setminus \mathcal{C}$, starting from $w^{(t)}$. Theorem 6 gives, upon using $\tau_t \geq \tau \geq 4\kappa \log(128 C_\theta \kappa)$,

$$\mathbb{E}\left[\|w_i^{(t+1)} - w_i^\star\|^2 \,\Big|\, \mathcal{E}, \mathcal{F}_t\right] \leq \frac{1}{64 C_\theta}\|w^{(t)} - w_i^\star\|^2 + \frac{8d\sigma^2}{\mu\tau_t} \, .$$

Note that $w^\star = (1/n)\sum_{j=1}^n H^{-1}H_j w_j^\star$, so that

$$\|w^\star - w_i^\star\| \leq \frac{1}{n}\sum_{j=1}^n \|H^{-1}H_j(w_j^\star - w_i^\star)\| \leq \Omega \, .$$

11

Algorithm 3 One-step Smoothed Weiszfeld Algorithm

Input: Same as Algorithm 2

1: Device i sets $\beta_i = \alpha_i/(\nu \vee \|w_i\|)$
2: **return** $\left(\sum_{i=1}^{m} \beta_i w_i\right)/\sum_{i=1}^{m} \beta_i$ using $\mathcal{A}$

Using $\|a + b\|^2 \le 2\|a\|^2 + 2\|b\|^2$, we get,

$$\mathbb{E}\left[\|w_i^{(t+1)} - w^\star\|^2 \,\big|\, \mathcal{E}, \mathcal{F}_t\right] \le 2\mathbb{E}\left[\|w_i^{(t+1)} - w_i^\star\|^2 \,\big|\, \mathcal{E}, \mathcal{F}_t\right] + 2\Omega^2$$

$$\le \frac{1}{32C_\theta}\|w^{(t)} - w_i^\star\|^2 + \frac{16d\sigma^2}{\mu\tau_t} + 2\Omega^2$$

$$\le \frac{q}{16C_\theta}\|w^{(t)} - w^\star\|^2 + \frac{16d\sigma^2}{\mu\tau_t} + 4\Omega^2 \,.$$

We now apply the robustness property of the GM ([59, Thm. 2.2] or [86, Lem. 3]) to get,

$$\mathbb{E}\left[\|w^{(t+1)} - w^\star\|^2 \,\big|\, \mathcal{E}, \mathcal{F}_t\right] \le \frac{1}{2}\|w^{(t)} - w^\star\|^2 + \frac{128C_\theta d\sigma^2}{\mu\tau_t} + \Gamma \,,$$

where $\Gamma = 2C_\theta(\epsilon^2/m^2 + 16\Omega^2)$. Taking an expectation conditioned on $\mathcal{E}$ and unrolling this inequality gives

$$\mathbb{E}\left[\|w^{(T)} - w^\star\|^2 \,\big|\, \mathcal{E}\right] \le \frac{\Delta_0}{2^T} + \frac{128C_\theta d\sigma^2}{\mu}\sum_{t=1}^{T}\frac{1}{2^{T-t}\tau_t} + 2\Gamma \,.$$

When $\tau_t = 2^t\tau$, the series sums to $2^{-(T-1)}T/\tau$, while for $\tau_t = \tau$, the series is upper bounded by $2/\tau$. $\quad\square$

We now consider RFA in connection with the three factors mentioned in Section 3.1.

(i) **Communication Efficiency**: Similar to FedAvg, RFA performs multiple local updates for each aggregation round, to save on the total communication. However, owing to the trade-off between communication, privacy and robustness, RFA requires a modest $3\times$ more communication for robustness per aggregation. In the next section, we present a heuristic to reduce this communication cost to one secure average oracle call per aggregation.

(ii) **Privacy Preservation**: Algorithm 2 computes the aggregation as an iterative secure aggregate. This means that the server only learns the intermediate parameters after being averaged over all the devices, with effective weights bounded away from 1 (Proposition 3). The noisy parameter vectors sent by individual devices are uniformly uninformative in information theoretic sense with the use of secure multi-party computation.

(iii) **Robustness**: The geometric median has a breakdown point of 1/2 [59, Theorem 2.2], which is the highest possible [59, Theorem 2.1]. In the federated learning context, this means that convergence is still guaranteed by Theorem 4 when up to half the points in terms of total weight are corrupted. RFA is resistant to both data or update poisoning, while being privacy preserving. On the other hand, FedAvg has a breakdown point of 0, where a single corruption in each round can cause the model to become arbitrarily bad.

4.2 Extensions to RFA

We now discuss two extensions to RFA to reduce the communication cost (without sacrificing privacy) and better accommodate statistical heterogeneity in the data with model personalization.

Algorithm 4 RFA with Personalization

Replace lines 4 to 8 of Algorithm 1 with the following:

1: Set $u_{i,0}^{(t)} = u_i^{(t)}$ and $w_{i,0}^{(t)} = w^{(t)}$

2: **for** $k = 0, \cdots, \tau - 1$ **do**

3:     $u_{i,k+1}^{(t)} = u_{i,k}^{(t)} - \gamma \nabla f(w^{(t)} + u_{i,k}^{(t)}; z_{i,k}^{(t)})$ with $z_{i,k}^{(t)} \sim D_i$

4: **for** $k = 0, \cdots, \tau - 1$ **do**

5:     $w_{i,k+1}^{(t)} = w_{i,k}^{(t)} - \gamma \nabla f(w_{i,k}^{(t)} + u_{i,\tau}^{(t)}; \tilde{z}_{i,k}^{(t)})$ with $\tilde{z}_{i,k}^{(t)} \sim D_i$

6: Set $w_i^{(t+1)} = w_{i,\tau}^{(t)}$ and $u_i^{(t+1)} = u_{i,\tau}^{(t)}$

One-step RFA: Reducing the Communication Cost. Recall that RFA results in a 3-5× increase in the communication cost over FedAvg. Here, we give a heuristic variant of RFA in an extremely communication-constrained setting, where it is infeasible to run multiple iterations of Algorithm 2. We simply run Algorithm 2 with $v^{(0)} = 0$ and a communication budget of $R = 1$; see Algorithm 3 for details. We find in Section 5.3 that one-step RFA retains most of the robustness of RFA.

Personalized RFA: Offsetting Heterogeneity. We now show RFA can be extended to better handle heterogeneity in the devices with the use of personalization. The key idea is that predictions are made on device i by summing the shared parameters w maintained by the server with personalized parameters $U = \{u_1, \cdots, u_n\}$ maintained individually on-device. In particular, the optimization problem we are interested in solving is

$$\min_{w,U} \left[F(w, U) := \sum_{i=1}^{n} \alpha_k \, \mathbb{E}_{z \sim D_i} \left[f(w + u_i; z) \right] \right] .$$

We outline the algorithm in Algorithm 4. We train the shared and personalized parameters on each other's residuals, following the residual learning scheme of [3]. Each selected device first updates its personalized parameters u_i while keeping the shared parameters w fixed. Next, the updates to the shared parameter are computed on the residual of the personalized parameters. The updates to the shared parameter are aggregated with the geometric median, identical to RFA. Experiments in Section 5.3 show that personalization is effective in combating heterogeneity.

5 Numerical Simulations

We now conduct simulations to compare RFA with other federated learning algorithms. The simulations were run using TensorFlow and the data was preprocessed using LEAF [19]. We first describe the experimental setup in Section 5.1, then study the robustness and convergence of RFA in Section 5.2. We study the effect of

Table 2: Dataset description and statistics.

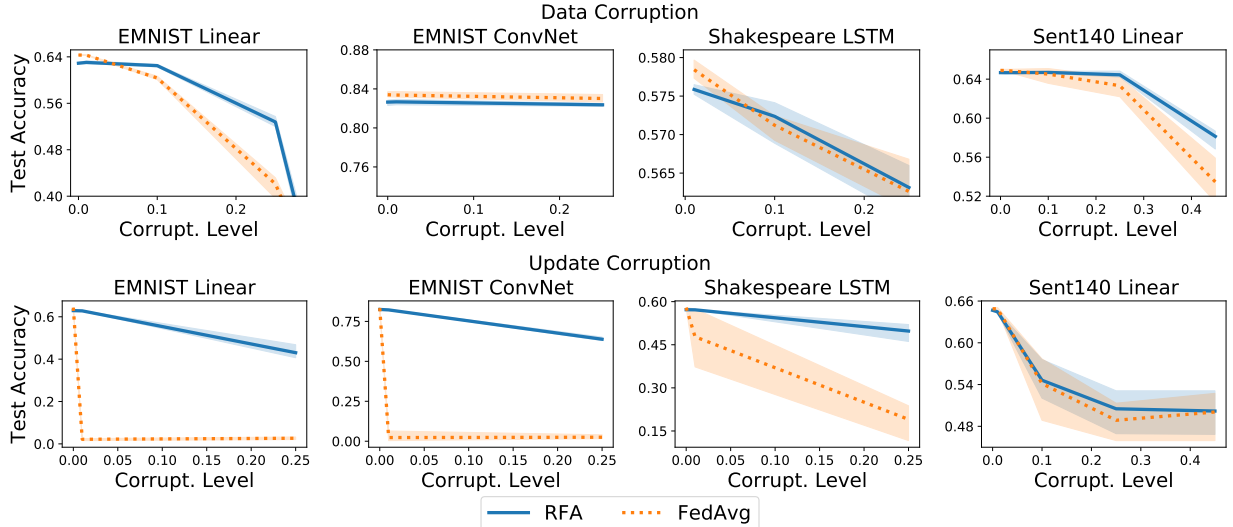| Dataset	Task	#Classes	#Train	#Test	#Devices	#Train per Device		
						Median	Max	Min
EMNIST	Image Classification	62	$204K$	$23K$	1000	160	418	92
Shakespeare	Character-level Language Modeling	53	$2.2M$	$0.25M$	628	1170	70600	90
Sent140	Sentiment Analysis	2	$57K$	$15K$	877	55	479	40

Figure 2: Comparison of robustness of RFA and FedAvg under data corruption (**top**) and update corruption (**bottom**). The left three plots for update corruption show omniscient corruption while the rightmost one shows Gaussian corruption. The shaded area denotes minimum and maximum over 5 random seeds.

the extensions of RFA in Section 5.3. The full details from this section and more simulation results are given in Appendix D. The code and scripts to reproduce these experiments can be found online [1].

5.1 Setup

We consider three machine learning tasks. The datasets are described in Table 2. As described in Section 3.1, we take the weight α_i of device i to be proportional to the number of datapoints N_i on the device.

(a) *Character Recognition*: We use the EMNIST dataset [26], where the input x is a 28×28 grayscale image of a handwritten character and the output y is its identification (0-9, a-z, A-Z). Each device is a writer of the handwritten character x. We use two models — a linear model $\varphi(x; w) = w^\top x$ and a convolutional neural network (ConvNet). We use as objective $f(w; (x, y)) = \ell(y, \varphi(x; w))$, where ℓ is the multinomial logistic loss ℓ. We evaluate performance using the classification accuracy.

(b) *Character-Level Language Modeling*: We learn a character-level language model over the Complete Works of Shakespeare [78]. We formulate it as a multiclass classification problem, where the input x is a window of 20 characters, the output y is the next (i.e., 21st) character. Each device is a role from a play (e.g., Brutus from The Tragedy of Julius Caesar). We use a long-short term memory model (LSTM) [38] together with the multinomial logistic loss. The performance is evaluated with the classification accuracy of next-character prediction.

(c) *Sentiment Analysis*: We use the Sent140 dataset [36] where the input x is a tweet and the output $y = \pm 1$ is its sentiment. Each device is a distinct Twitter user. We use a linear model using average of the GloVe embeddings [74] of the words of the tweet. It is trained with the binary logistic loss and evaluated with the classification accuracy.

Corruption Models. We consider the following corruption models for corrupted devices $\mathcal{C}$, cf. Section 3.2:

(a) *Data Poisoning*: The distribution D_i on a device $k \in \mathcal{C}$ is replaced by some fixed $\tilde{D}_i$. For EMNIST, we take the negative of an image so that $\tilde{D}_i(x, y) = D_i(1 - x, y)$. For the Shakespeare dataset, we reverse the text so that $\tilde{D}_i(c_1, \cdots c_{20}, c_{21}) = D_i(c_{21}, \cdots c_2, c_1)$. In both these cases, the labels are unchanged. For the Sent140 dataset, we flip the label while keeping x unchanged.
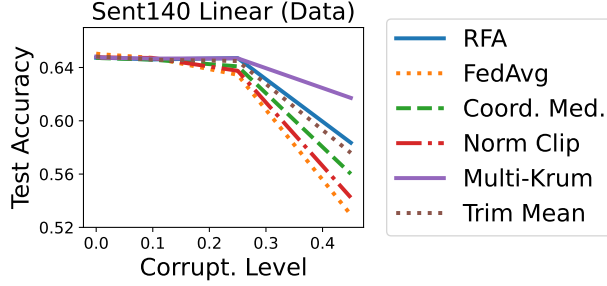
14

Figure 3: Comparison of RFA with other robust aggregation algorithms on Sent140 with data corruption.

(b) *Update poisoning with Gaussian corruption*: Each corrupted device $i \in \mathcal{C}$ returns $w_i^{(t+1)} = w_{i,\tau}^{(t)} + \zeta_i^{(t)}$, where $\zeta_i^{(t)} \sim \mathcal{N}(0, \sigma^2 I)$, where σ^2 is the variance across the components of $w_{i,\tau}^{(t)} - w^{(t)}$.[2]

(c) *Update poisoning with omniscient corruption*: The parameters $w_i^{(t+1)}$ returned by devices $i \in \mathcal{C}$ are modified so that the weighted arithmetic mean $\sum_{i \in S_t} \alpha_i w_i^{(t+1)}$ over the selected devices S_t is set to $-\sum_{i \in S_t} \alpha_i w_{i,\tau}^{(t)}$, the negative of what it would to have been without the corruption. This is designed to hurt the weighted arithmetic mean aggregation.

Hyperparameters. The hyperparameters are chosen similar to the defaults of [66]. A learning rate schedule was tuned on a validation set for FedAvg with no corruption. The same schedule was used for RFA. The aggregation in RFA is implemented using the smoothed Weiszfeld algorithm with a budget of $R = 3$ calls to the secure average oracle, thanks to its rapid empirical convergence (cf. Figure 1), and $\nu = 10^{-6}$ for numerical stability. Each simulation was repeated 5 times and the shaded area denotes the minimum and maximum over these runs. Appendix D gives details on hyperparameter, and a sensitivity analysis of the Weiszfeld communication budget.

5.2 Robustness and Convergence of RFA

First, we compare the robustness of RFA as opposed to vanilla FedAvg to different types of corruption across different datasets in Figure 2. We make the following observations.

RFA gives improved robustness to linear models with data corruption. For instance, consider the EMNIST linear model at $\rho = 1/4$. RFA achieves 52.8% accuracy, over 10% better than FedAvg at 41.2%.

RFA performs similarly to FedAvg in deep nets with data corruption. RFA and FedAvg are within one standard deviations of each other for the Shakespeare LSTM model, and nearly equal for the EMNIST ConvNet model. We note that the behavior of the training of a neural network when the data is corrupted is not well-understood in general [e.g., 90].

RFA gives improved robustness to omniscient corruptions for all models. For the omniscient corruption, the test accuracy of the FedAvg is close to 0% for the EMNIST linear model and ConvNet, while RFA still achieves over 40% at $\rho = 1/4$ for the former and well over 60% for the latter. A similar trend holds for the Shakespeare LSTM model.

RFA almost matches FedAvg in the absence of corruption. Recall from Section 3.2 that robustness comes at the cost of heterogeneity; this is also reflected in the theory of Section 4. Empirically, we find that the performance hit of RFA due to heterogeneity is quite small: 1.4% for the EMNIST linear model (64.3%

---

[2]Model updates $w_i^{(t)} - w^{(t)}$ are aggregated, not the models $w_i^{(t)}$ directly [46].
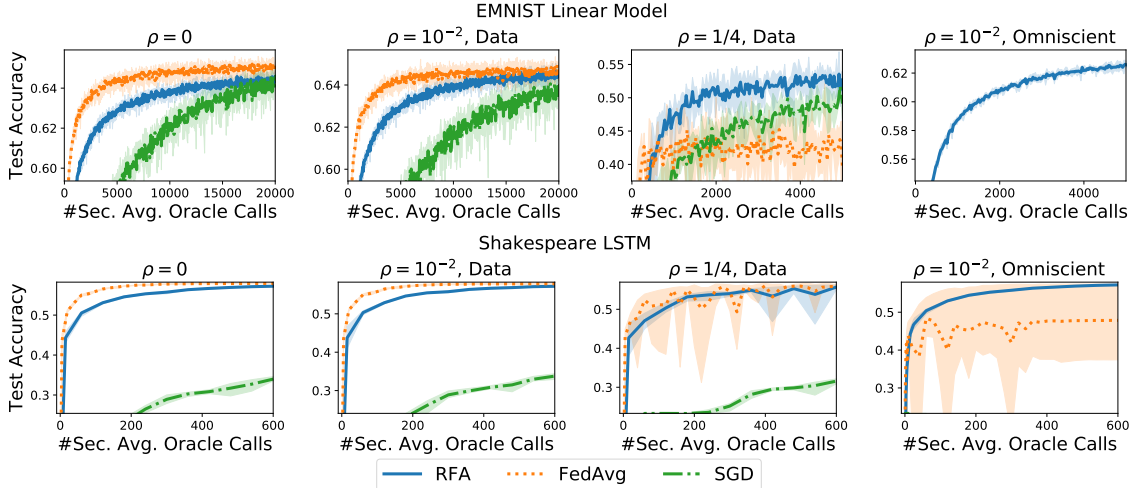
Figure 4: Comparison of methods plotted against number of calls to the secure average oracle for different corruption settings. For the case of omniscient corruption, FedAvg and SGD are not shown in the plot if they diverge. The shaded area denotes the maximum and minimum over 5 random seeds.
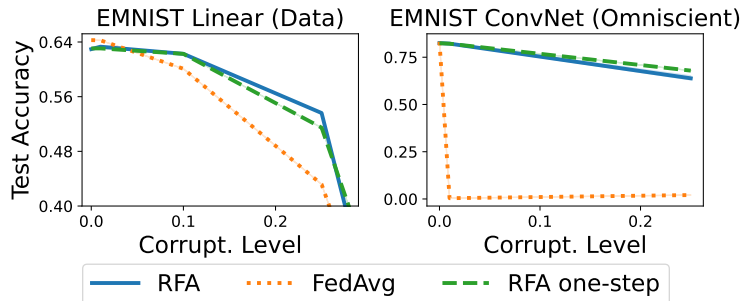

Figure 5: Robustness of one-step RFA.

vs. 62.9%), under 0.4% for the Shakespeare LSTM, and 0.3% for Sent140 (65.0% vs. 64.7%). Further, we demonstrate in Appendix D.5 that, consistent with the theory, this gap completely vanishes in the i.i.d. case.

RFA is competitive with other robust aggregation schemes while being privacy-preserving. We now compare RFA with: (a) coordinate-wise median [88] and ℓ_2 norm clipping [82] which are agnostic to the actual corruption level ρ like RFA, and, (b) trimmed mean [88] and multi-Krum [16], that require exact knowledge of the level of corruption ρ in the problem. We find that RFA is more robust than the two agnostic algorithms coordinate-wise median and norm clipping. Perhaps surprisingly, RFA is also more robust than the trimmed mean which uses perfect knowledge of the corruption level ρ. We note that multi-Krum is more robust than RFA. That being said, RFA has the advantage that it is fully agnostic to the actual corruption level ρ and is privacy-preserving, while the other robust approaches are not.

Summary: robustness of RFA. Overall, we find that RFA is no worse than FedAvg in the presence of corruption and is often better, while being almost as good in the absence of corruption. Furthermore, RFA degrades more gracefully as the corruption level increases.

RFA requires only $3\times$ the communication of FedAvg. Next, we plot in Figure 4 the performance versus the number of rounds of communication as measured by the number of calls to the secure average oracle. We note that in the low corruption regime of $\rho = 0$ or $\rho = 10^{-2}$ under data corruption, RFA requires
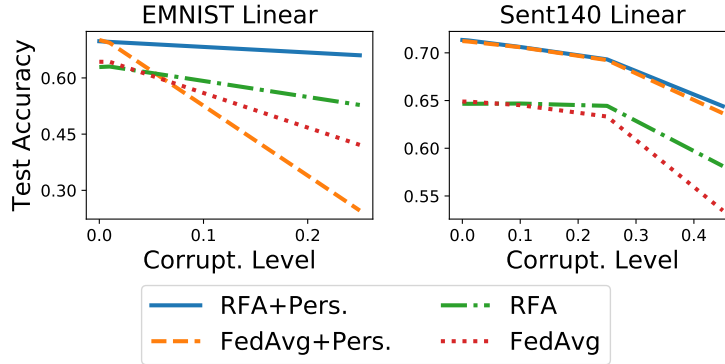
Figure 6: Effect of personalization on the robustness of RFA and FedAvg under data corruption.

$3\times$ the number of calls to the secure average oracle to reach the same performance. However, it matches the performance of FedAvg when measured in terms of the number of outer iterations, with the additional communication cost coming from multiple Weiszfeld iterations for computation of the average.

RFA exhibits more stable convergence under corruption. We also see from Figure 4 ($\rho = 1/4$, Data) that the variability of accuracy across random runs, denoted here by the shaded region, is much smaller for RFA. Indeed, by being robust to the corrupted updates sent by random sampling of corrupted clients, RFA exhibits a more stable convergence across iterations.

5.3 Extensions of RFA

We now study the proposed extensions: one-step RFA and personalization.

One-step RFA gives most of the robustness with no extra communication. From Figure 5, we observe that for one-step RFA is quite close in performance to RFA across different levels of corruption for both data corruption on an EMNIST linear model and omniscient corruption on an EMNIST ConvNet. For instance, in the former, one-step RFA gets 51.4% in accuracy, which is 10% better than FedAvg while being almost as good as full RFA (52.8%) at $\rho = 0.25$. Moreover, for the latter, we find that one-step RFA (67.9%) actually achieves higher test accuracy than full RFA (63.0%) at $\rho = 0.25$.

Personalization helps RFA offset effects of heterogeneity. Figure 6 plots the effect of RFA with personalization. First, we observe that personalization leads to an improvement with no corruption for both FedAvg and RFA. For the EMNIST linear model, we get 70.1% and 69.9% respectively from 64.3% and 62.9%. Second, we observe that RFA exhibits greater robustness to corruption with personalization. At $\rho = 1/4$ with the EMNIST linear model, RFA with personalization gives 66.4% (a reduction of 3.4%) while no personalization gives 52.8% (a reduction of 10.1%). The results for Sent140 are similar, with the exception that FedAvg with personalization is nearly identical to RFA with personalization.

6 Conclusion

We presented a robust aggregation approach, based on the geometric median and the smoothed Weiszfeld algorithm to efficiently compute it, to make federated learning more robust to settings where a fraction of the devices may be sending corrupted updates to the orchestrating server. The robust aggregation oracle preserves the privacy of participating devices, operating with calls to secure multi-party computation primitives enjoying privacy preservation theoretical guarantees. RFA is available in several variants, including a fast one with a single step of robust aggregation and a one adjusting to heterogeneity with on-device personalization. All

variants are readily scalable while preserving privacy, building off secure multi-party computation primitives already used at planetary scale. The theoretical analysis of RFA with personalization is an interesting venue for future work. The further analysis of robustness under heterogeneity is also an interesting venue for future work.

Acknowledgments

References

[1] `https://github.com/krishnap25/rfa`, 2019.

[2] `https://github.com/google-research/federated/tree/master/robust_aggregation`, 2019.

[3] A. Agarwal, J. Langford, and C.-Y. Wei. Federated Residual Learning. *arXiv Preprint*, 2020.

[4] S. Al-Sayed, A. M. Zoubir, and A. H. Sayed. Robust Distributed Estimation by Networked Agents. *IEEE Transactions on Signal Processing*, 65(15):3909–3921, 2017.

[5] D. Alistarh, Z. Allen-Zhu, and J. Li. Byzantine Stochastic Gradient Descent. In *Advances in Neural Information Processing Systems 31*, pages 4618–4628, 2018.

[6] M. Ammad-ud din, E. Ivannikova, S. A. Khan, W. Oyomno, Q. Fu, K. E. Tan, and A. Flanagan. Federated Collaborative Filtering for Privacy-Preserving Personalized Recommendation System. *arXiv Preprint*, 2019.

[7] D. Avdiukhin and S. P. Kasiviswanathan. Federated Learning under Arbitrary Communication Patterns. In *International Conference on Machine Learning*, volume 139 of *Proceedings of Machine Learning Research*, pages 425–435. PMLR, 2021.

[8] F. Bach and E. Moulines. Non-strongly-convex smooth stochastic approximation with convergence rate $O(1/n)$. In *Advances in Neural Information Processing Systems*, pages 773–781, 2013.

[9] B. Balle, G. Barthe, M. Gaboardi, J. Hsu, and T. Sato. Hypothesis Testing Interpretations and Renyi Differential Privacy. In *The 23rd International Conference on Artificial Intelligence and Statistics, AISTATS 2020, 26-28 August 2020, Online [Palermo, Sicily, Italy]*, volume 108 of *Proceedings of Machine Learning Research*, pages 2496–2506. PMLR, 2020.

[10] A. Beck. On the Convergence of Alternating Minimization for Convex Programming with Applications to Iteratively Reweighted Least Squares and Decomposition Schemes. *SIAM Journal on Optimization*, 25(1):185–209, 2015.

[11] A. Beck and S. Sabach. Weiszfeld's Method: Old and New Results. *J. Optimization Theory and Applications*, 164(1):1–40, 2015.

[12] A. Beck and M. Teboulle. Smoothing and First Order Methods: A Unified Framework. *SIAM Journal on Optimization*, 22(2):557–580, 2012.

[13] J. H. Bell, K. A. Bonawitz, A. Gascón, T. Lepoint, and M. Raykova. Secure Single-Server Aggregation with (Poly)Logarithmic Overhead. In *ACM SIGSAC Conference on Computer and Communications Security*, pages 1253–1269, 2020.

[14] D. P. Bertsekas. *Nonlinear Programming*. Athena Scientific, 1999.

[15] D. P. Bertsekas and J. N. Tsitsiklis. *Parallel and Distributed Computation: Numerical Methods*, volume 23. Prentice hall Englewood Cliffs, NJ, 1989.

[16] P. Blanchard, R. Guerraoui, E. M. El Mhamdi, and J. Stainer. Machine learning with adversaries: Byzantine tolerant gradient descent. In *Advances in Neural Information Processing Systems 30*, pages 119–129, 2017.

[17] K. Bonawitz, V. Ivanov, B. Kreuter, A. Marcedone, H. B. McMahan, S. Patel, D. Ramage, A. Segal, and K. Seth. Practical Secure Aggregation for Privacy-Preserving Machine Learning. In *ACM SIGSAC Conference on Computer and Communications Security*, pages 1175–1191, 2017.

[18] K. A. Bonawitz, H. Eichner, W. Grieskamp, D. Huba, A. Ingerman, V. Ivanov, C. Kiddon, J. Konečný, S. Mazzocchi, B. McMahan, T. V. Overveldt, D. Petrou, D. Ramage, and J. Roselander. Towards Federated Learning at Scale: System Design. In *Proceedings of Machine Learning and Systems*, 2019.

[19] S. Caldas, P. Wu, T. Li, J. Konečný, H. B. McMahan, V. Smith, and A. Talwalkar. LEAF: A benchmark for federated settings. *arXiv Preprint*, 2018.

[20] X. Cao and L. Lai. Distributed Gradient Descent Algorithm Robust to an Arbitrary Number of Byzantine Attackers. *IEEE Transactions on Signal Processing*, 67(22):5850–5864, 2019.

[21] L. Chen, H. Wang, Z. Charles, and D. Papailiopoulos. DRACO: Byzantine-resilient Distributed Training via Redundant Gradients. In *International Conference on Machine Learning*, pages 902–911, 2018.

[22] M. Chen, C. Gao, and Z. Ren. Robust Covariance and Scatter Matrix Estimation under Huber's Contamination Model. *Annals of Statistics*, 46(5):1932–1960, 2018.

[23] Y. Chen, L. Su, and J. Xu. Distributed Statistical Machine Learning in Adversarial Settings: Byzantine Gradient Descent. *Proceedings of the ACM on Measurement and Analysis of Computing Systems*, 1(2): 44, 2017.

[24] Y. Chen, S. Kar, and J. M. Moura. Resilient Distributed Parameter Estimation With Heterogeneous Data. *IEEE Transactions on Signal Processing*, 67(19):4918–4933, 2019.

[25] Y. Cheng, I. Diakonikolas, and R. Ge. High-Dimensional Robust Mean Estimation in Nearly-Linear Time. In *ACM-SIAM Symposium on Discrete Algorithms*, pages 2755–2771, 2019.

[26] G. Cohen, S. Afshar, J. Tapson, and A. van Schaik. EMNIST: an extension of MNIST to handwritten letters. *arXiv Preprint*, 2017.

[27] M. B. Cohen, Y. T. Lee, G. L. Miller, J. Pachocki, and A. Sidford. Geometric Median in Nearly Linear Time. In *Symposium on Theory of Computing*, pages 9–21, 2016.

[28] I. Diakonikolas, G. Kamath, D. M. Kane, J. Li, A. Moitra, and A. Stewart. Robust Estimators in High Dimensions without the Computational Intractability. In *Symposium on Foundations of Computer Science*, pages 655–664, 2016.

[29] C. T. Dinh, N. H. Tran, and T. D. Nguyen. Personalized Federated Learning with Moreau Envelopes. In H. Larochelle, M. Ranzato, R. Hadsell, M. Balcan, and H. Lin, editors, *Advances in Neural Information Processing Systems 33*, 2020.

[30] D. L. Donoho and P. J. Huber. The notion of breakdown point. *A festschrift for Erich L. Lehmann*, 157184, 1983.

[31] C. Dwork, F. McSherry, K. Nissim, and A. D. Smith. Calibrating Noise to Sensitivity in Private Data Analysis. In *Theory of Cryptography Conference*, volume 3876 of *Lecture Notes in Computer Science*, pages 265–284. Springer, 2006.

[32] D. Evans, V. Kolesnikov, M. Rosulek, et al. A Pragmatic Introduction to Secure Multi-Party Computation. *Foundations and Trends in Privacy and Security*, 2(2-3):70–246, 2018.

[33] A. Fallah, A. Mokhtari, and A. E. Ozdaglar. Personalized Federated Learning with Theoretical Guarantees: A Model-Agnostic Meta-Learning Approach. In *Advances in Neural Information Processing Systems*, 2020.

[34] T. Gafni, N. Shlezinger, K. Cohen, Y. C. Eldar, and H. V. Poor. Federated Learning: A Signal Processing Perspective. *arXiv Preprint*, 2021.

[35] C. Gentry. Computing arbitrary functions of encrypted data. *Commun. ACM*, 53(3):97–105, 2010.

[36] A. Go, R. Bhayani, and L. Huang. Twitter Sentiment Classification using Distant Supervision. *CS224N Project Report, Stanford*, page 2009, 2009.

[37] L. He, A. Bian, and M. Jaggi. COLA: Decentralized Linear Learning. In *Advances in Neural Information Processing Systems 31*, pages 4541–4551, 2018.

[38] S. Hochreiter and J. Schmidhuber. Long Short-Term Memory. *Neural computation*, 9(8):1735–1780, 1997.

[39] D. J. Hsu and S. Sabato. Loss Minimization and Parameter Estimation with Heavy Tails. *Journal of Machine Learning Research*, 17:18:1–18:40, 2016.

[40] L. Huang, A. L. Shea, H. Qian, A. Masurkar, H. Deng, and D. Liu. Patient Clustering Improves Efficiency of Federated Machine Learning to Predict Mortality and Hospital stay time using Distributed Electronic Medical Records. *Journal of Biomedical Informatics*, 99:103291, 2019.

[41] P. J. Huber. Robust estimation of a location parameter. *The Annals of Mathematical Statistics*, 35(1): 73–101, 03 1964.

[42] P. J. Huber. *Robust Statistics*. Springer, 2011.

[43] P. Jain, S. M. Kakade, R. Kidambi, P. Netrapalli, V. K. Pillutla, and A. Sidford. A Markov Chain Theory Approach to Characterizing the Minimax Optimality of Stochastic Gradient Descent (for Least Squares). In *Conference on Foundations of Software Technology and Theoretical Computer Science*, pages 2:1–2:10, 2017.

[44] P. Jain, S. M. Kakade, R. Kidambi, P. Netrapalli, and A. Sidford. Parallelizing stochastic gradient descent for least squares regression: Mini-batching, averaging, and model misspecification. *Journal of Machine Learning Research*, 18:223:1–223:42, 2017.

[45] P. Kairouz, Z. Liu, and T. Steinke. The Distributed Discrete Gaussian Mechanism for Federated Learning with Secure Aggregation. In *ICML*, volume 139, pages 5201–5212, 2021.

[46] P. Kairouz, H. B. McMahan, B. Avent, A. Bellet, M. Bennis, A. N. Bhagoji, K. A. Bonawitz, Z. Charles, G. Cormode, R. Cummings, R. G. L. D'Oliveira, H. Eichner, S. E. Rouayheb, D. Evans, J. Gardner, Z. Garrett, A. Gascón, B. Ghazi, P. B. Gibbons, M. Gruteser, Z. Harchaoui, C. He, L. He, Z. Huo, B. Hutchinson, J. Hsu, M. Jaggi, T. Javidi, G. Joshi, M. Khodak, J. Konečný, A. Korolova, F. Koushanfar, S. Koyejo, T. Lepoint, Y. Liu, P. Mittal, M. Mohri, R. Nock, A. Özgür, R. Pagh, H. Qi, D. Ramage, R. Raskar, M. Raykova, D. Song, W. Song, S. U. Stich, Z. Sun, A. T. Suresh, F. Tramèr, P. Vepakomma, J. Wang, L. Xiong, Z. Xu, Q. Yang, F. X. Yu, H. Yu, and S. Zhao. Advances and Open Problems in Federated Learning. *Found. Trends Mach. Learn.*, 14(1-2):1–210, 2021.

[47] S. P. Karimireddy, S. Kale, M. Mohri, S. Reddi, S. Stich, and A. T. Suresh. Scaffold: Stochastic Controlled Averaging for Federated Learning. In *International Conference on Machine Learning*, pages 5132–5143. PMLR, 2020.

[48] I. N. Katz. Local convergence in Fermat's problem. *Mathematical Programming*, 6(1):89–104, 1974.

[49] H. W. Kuhn. A note on Fermat's problem. *Mathematical Programming*, 4(1):98–107, Dec 1973.

[50] Y. Laguel, K. Pillutla, J. Malick, and Z. Harchaoui. A Superquantile Approach to Federated Learning with Heterogeneous Devices. In *Conference on Information Sciences and Systems*, pages 1–6. IEEE, 2021.

[51] L. Lamport, R. E. Shostak, and M. C. Pease. The Byzantine Generals Problem. *ACM Trans. Program. Lang. Syst.*, 4(3):382–401, 1982.

[52] R. Leblond, F. Pedregosa, and S. Lacoste-Julien. Improved Asynchronous Parallel Optimization Analysis for Stochastic Incremental Methods. *Journal of Machine Learning Research*, 19, 2018.

[53] G. Lecué and M. Lerasle. Robust machine learning by median-of-means: Theory and practice. *The Annals of Statistics*, 48(2):906–931, 2020.

[54] Y. LeCun, L. Bottou, Y. Bengio, P. Haffner, et al. Gradient-Based Learning Applied to Document Recognition. *Proceedings of the IEEE*, 86(11):2278–2324, 1998.

[55] L. Li, W. Xu, T. Chen, G. B. Giannakis, and Q. Ling. RSA: Byzantine-Robust Stochastic Aggregation Methods for Distributed Learning from Heterogeneous Datasets. In *AAAI Conference on Artificial Intelligence*, pages 1544–1551. AAAI Press, 2019.

[56] T. Li, A. K. Sahu, A. Talwalkar, and V. Smith. Federated Learning: Challenges, Methods, and Future Directions. *IEEE Signal Processing Magazine*, 37(3):50–60, 2020.

[57] T. Li, A. K. Sahu, M. Zaheer, M. Sanjabi, A. Talwalkar, and V. Smith. Federated Optimization in Heterogeneous Networks. In *Proceedings of Machine Learning and Systems*, 2020.

[58] S. Lin, G. Yang, and J. Zhang. A Collaborative Learning Framework via Federated Meta-Learning. In *IEEE International Conference on Distributed Computing Systems*, pages 289–299. IEEE, 2020.

[59] H. P. Lopuhaa and P. J. Rousseeuw. Breakdown points of affine equivariant estimators of multivariate location and covariance matrices. *Annals of Statistics*, 19(1):229–248, 03 1991.

[60] G. Lugosi and S. Mendelson. Regularization, sparse recovery, and median-of-means tournaments. *arXiv Preprint*, 2017.

[61] G. Lugosi and S. Mendelson. Risk minimization by median-of-means tournaments. *Journal of the European Mathematical Society*, 22(3):925–965, 2019.

[62] C. Ma, J. Konečný, M. Jaggi, V. Smith, M. I. Jordan, P. Richtárik, and M. Takác. Distributed optimization with arbitrary local solvers. *Optimization Methods and Software*, 32(4):813–848, 2017.

[63] J. Mairal. Optimization with First-Order Surrogate Functions. In *International Conference on Machine Learning*, pages 783–791, 2013.

[64] J. Mairal. Incremental Majorization-Minimization Optimization with Application to large-scale machine learning. *SIAM Journal on Optimization*, 25(2):829–855, 2015.

[65] R. Maronna, D. Martin, and V. Yohai. *Robust Statistics: Theory and Methods*. Wiley, 2006.

[66] B. McMahan, E. Moore, D. Ramage, S. Hampson, and B. A. y Arcas. Communication-Efficient Learning of Deep Networks from Decentralized Data. In *Artificial Intelligence and Statistics*, pages 1273–1282, 2017.

[67] S. Minsker. Geometric median and robust estimation in Banach spaces. *Bernoulli*, 21(4):2308–2335, 2015.

[68] S. Minsker. Uniform Bounds for Robust Mean Estimators. *arXiv Preprint*, 2018.

[69] M. Mohri, G. Sivek, and A. T. Suresh. Agnostic Federated Learning. In *International Conference on Machine Learning*, volume 97, pages 4615–4625, 2019.

[70] A. S. Nemirovski and D. B. Yudin. Problem Complexity and Method Efficiency in Optimization. 1983.

[71] Y. Nesterov. *Introductory Lectures on Convex Optimization Vol. I: Basic course*, volume 87. Springer Science & Business Media, 2013.

[72] V. M. Panaretos and Y. Zemel. *An Invitation to Statistics in Wasserstein Space*. Springer Nature, 2020.

[73] A. Pantelopoulos and N. G. Bourbakis. A Survey on Wearable Sensor-Based Systems for Health Monitoring and Prognosis. *IEEE Transactions on Systems, Man, and Cybernetics, Part C (Applications and Reviews)*, 40(1):1–12, 2009.

[74] J. Pennington, R. Socher, and C. D. Manning. GloVe: Global Vectors for Word Representation. In *Empirical Methods in Natural Language Processing*, pages 1532–1543, 2014.

[75] S. J. Reddi, Z. Charles, M. Zaheer, Z. Garrett, K. Rush, J. Konečný, S. Kumar, and H. B. McMahan. Adaptive Federated Optimization. In *International Conference on Learning Representations*, 2021.

[76] J. Ren, H. Wang, T. Hou, S. Zheng, and C. Tang. Federated Learning-Based Computation Offloading Optimization in Edge Computing-Supported Internet of Things. *IEEE Access*, 7:69194–69201, 2019.

[77] A. H. Sayed. Adaptation, Learning, and Optimization over Networks. *Foundations and Trends in Machine Learning*, 7(4-5):311–801, 2014.

[78] W. Shakespeare. The Complete Works of William Shakespeare. URL `https://www.gutenberg.org/ebooks/100`.

[79] V. Smith, C.-K. Chiang, M. Sanjabi, and A. S. Talwalkar. Federated multi-task learning. In *Advances in Neural Information Processing Systems 30*, pages 4424–4434, 2017.

[80] V. Smith, S. Forte, M. Chenxin, M. Takáč, M. I. Jordan, and M. Jaggi. COCOA: A General Framework for Communication-Efficient Distributed Optimization. *Journal of Machine Learning Research*, 18:230, 2018.

[81] P. Subramanyan, R. Sinha, I. Lebedev, S. Devadas, and S. A. Seshia. A Formal Foundation for Secure Remote Execution of Enclaves. In *ACM SIGSAC Conference on Computer and Communications Security*, pages 2435–2450, 2017.

[82] Z. Sun, P. Kairouz, A. T. Suresh, and H. B. McMahan. Can You Really Backdoor Federated Learning? *arXiv Preprint*, 2019.

[83] Y. Vardi and C.-H. Zhang. A modified Weiszfeld algorithm for the Fermat-Weber location problem. *Mathematical Programming*, 90(3):559–566, 2001.

[84] J. Wang, Z. Charles, Z. Xu, G. Joshi, H. B. McMahan, M. Al-Shedivat, G. Andrew, S. Avestimehr, K. Daly, D. Data, et al. A Field Guide to Federated Optimization. *arXiv Preprint*, 2021.

[85] E. Weiszfeld. Sur le point pour lequel la somme des distances de n points donnés est minimum. *Tohoku Mathematical Journal, First Series*, 43:355–386, 1937.

[86] Z. Wu, Q. Ling, T. Chen, and G. B. Giannakis. Federated variance-reduced stochastic gradient descent with robustness to byzantine attacks. *IEEE Transactions on Signal Processing*, 68:4583–4596, 2020.

[87] T. Yang, G. Andrew, H. Eichner, H. Sun, W. Li, N. Kong, D. Ramage, and F. Beaufays. Applied Federated Learning: Improving Google Keyboard Query Suggestions. *arXiv preprint arXiv:1812.02903*, 2018.

[88] D. Yin, Y. Chen, K. Ramchandran, and P. Bartlett. Byzantine-robust distributed learning: Towards optimal statistical rates. In *International Conference on Machine Learning*, pages 5636–5645, 2018.

[89] Y. Yu, H. Zhao, R. C. de Lamare, Y. Zakharov, and L. Lu. Robust Distributed Diffusion Recursive Least Squares Algorithms with Side Information for Adaptive Networks. *IEEE Transactions on Signal Processing*, 67(6):1566–1581, 2019.

[90] C. Zhang, S. Bengio, M. Hardt, B. Recht, and O. Vinyals. Understanding deep learning requires rethinking generalization. In *International Conference on Learning Representations*, 2017.

[91] W. Zhuang, X. Gan, Y. Wen, S. Zhang, and S. Yi. Collaborative Unsupervised Visual Representation Learning from Decentralized Data. In *ICCV*, pages 4912–4921, 2021.

Supplementary Material:
Robust Aggregation for Federated Learning

Table of Contents

A Table of Notation

We summarize the notation used throughout the paper in Table 3.

Table 3: Summary of notation.

Context	Symbol	Meaning
Setup	n	Total number of devices
	α_i	The weight of device i
	D_i	Data distribution of device i
	$\mathcal{D}$	Family of probability distributions such that $D_i \in \mathcal{D}$ for each non-corrupted device
	$\mathrm{width}(\mathcal{D})$	Degree of heterogeneity in $\mathcal{D}$
	z	Random variable denoting the data $z \sim D_i$. For example, $z = (x, y)$ is an input-output pair for supervised learning
	w	Model parameters in $\mathbb{R}^d$
	$f(w; z)$	Loss of model w on example z
	$F(w)$	Average objective across all devices; defined in Eq. (1)
	$w^\star$	Optimal model parameters $w^\star = \arg\min_{w \in \mathbb{R}^d} F(w)$
FL algorithms	m	Number of devices chosen per round for federated learning
	t	index of outer iteration of RFA or FedAvg
	S_t	Random subset of m devices chosen from $\{1, \cdots, n\}$ in round t
	$w^{(t)}$	Global model in round t
	$w_{i,k}^{(t)}$	Local updates on device i in round t for $k = 1, \cdots, \tau$
	$w_i^{(t+1)}$	Updated parameter returned by a selected client $i \in S_t$ in round t
Corruption models	$\mathcal{C}$	Subset of clients which send corrupted updates; $\mathcal{C} \subseteq [n]$
	ρ	Corruption level, defined as the fraction $\sum_{i \in \mathcal{C}} \alpha_i / \sum_{i \in [n]} \alpha_i$
	$\tilde{D}_i$	Distribution on device i due to static data poisoning, different from the original D_i
Geometric median definition	v	Vector in $\mathbb{R}^d$; used to denote the current estimates of the geometric median
	g	Geometric median (GM) objective, whose minimizer is the GM
	ϵ	Approximation tolerance of the GM
	ν	Smoothing parameter for the geometric median objective
	η	Auxiliary variables used to define a surrogate G
	G	Surrogate to the geometric median objective using auxiliary variables η
Convergence of RFA	x	Input component of z to make a prediction; input on device i is denoted x_i
	y	Output component of z which is the target prediction; output on device i is denoted y_i
	$\phi(x)$	d-dimensional feature map (i.e., basis) used for linear model $\phi(x)^\top w$
	ℓ	Loss function, so that $f(w; \xi) = \ell(y, \phi(x)^\top w)$, where $\xi = (x, y)$ is the data. We take ℓ to the least-squares loss for the theory
	$F_i(w)$	Local objective on device i
	$w_i^\star$	Local optimum of device i, i.e., $w_i^\star = \arg\min_w F_i(w)$
	$D_{X,i}$	Marginal distribution of D_i over the x-component of the data
	$D_{Y|X,i}$	Conditional distribution of y given x on device i; $D_i = D_{X,i} \otimes D_{Y|X,i}$
	R	Bound on the norm of the feature map $R \geq \|\phi(x)\|$
	L	Smoothness of each local objective F_i
	μ	Strong convexity of each local objective F_i
	κ	Condition number $\kappa = R^2/\mu$
	σ^2	Noise variance in the linear model
	H_i	Hessian $\nabla^2 F_i(w)$ on each device i; note that it is constant for all w
	H	Hessian $\nabla^2 F(w)$ of the average global objective F; we have, $H_k = (1/n) \sum_{i=1}^K \nabla^2 F_i(w)$
	Ω_X	Degree of heterogeneity in the marginal distributions $D_{X,k}$ over x; cf. Eq. (8)
	$\Omega_{Y|X}$	Degree of heterogeneity in the condition distribution $D_{Y|X,k}$ of $y|x$; cf. Eq. (8)
	Ω	Shorthand of $\mathrm{width}(\mathcal{D}_k)$, which denotes the degree of heterogeneity in D_k; defined as $\Omega = \Omega_X \Omega_{Y|X}$
	γ	Learning rate of SGD
	τ_t	Number of local steps of SGD on each device in outer FL round t
	δ	Confidence parameter in $(0, 1)$
	T	Number of rounds of federated learning
Personalization	u_i	Personalization parameter of device i; it is a vector in $\mathbb{R}^d$

B Template Implementation of RFA in TensorFlow Federated

We provide here a template implementation of RFA in Tensorflow Federated. The open source software is publicly available [2].

Listing 1: Template implementation of RFA in Tensorflow Federated

```python
# Code for dataset setup, model setup, etc. comes here
federated_train_data = ...
model_fn = ... # See e.g., TFF tutorials

# Running FedAvg in TFF
import tensorflow_federated as tff
iterative_process = tff.learning.build_federated_averaging_process(model_fn)
state = iterative_process.initialize()
for round_num in range(1, num_rounds):
    state, metrics = iterative_process.next(state, federated_train_data)


# Running RFA
from federated_research.robust_aggregation import build_robust_federated_aggregation_proc
iterative_process = build_robust_federated_aggregation_process(model_fn)
# Rest of the code remains unchanged
state = iterative_process.initialize()
for round_num in range(1, num_rounds):
    state, metrics = iterative_process.next(state, federated_train_data)
```

C The Smoothed Weiszfeld Algorithm: Convergence Analysis

In this section, we prove the rate of the smoothed Weiszfeld algorithm in Proposition 2. We start by a setup, prove a number of interesting properties, and finally prove Proposition 2 in Appendix C.5.

C.1 Setup

We are given distinct points $w_1, \cdots, w_m \in \mathbb{R}^d$ and scalars $\alpha_1, \cdots, \alpha_m > 0$ such that $\sum_{i=1}^m \alpha_i = 1$. We make the following non-degenerateness assumption, which is assumed to hold throughout this work. It is reasonable in the federated learning setting we consider.

Assumption 7. *The points $w_1, \cdots, w_i$ are not collinear.*

The geometric median is defined as any minimizer of

$$g(z) := \sum_{i=1}^m \alpha_i \|z - w_i\|. \tag{10}$$

Under Assumption 7, g is known to have a unique minimizer - we denote it by $z^\star$.

Given a smoothing parameter $\nu > 0$, its smoothed variant g_ν is

$$g_\nu(z) := \sum_{i=1}^m \alpha_i \|z - w_i\|_{(\nu)}, \tag{11}$$

Algorithm 5 The Smoothed Weiszfeld Algorithm

Input: $w_1, \cdots, w_m \in \mathbb{R}^d$, $\alpha_1, \cdots, \alpha_m > 0$ with $\sum_{i=1}^m \alpha_i = 1$, $\nu > 0$, number of iterations R, $v^{(0)} \in$ conv$\{w_1, \cdots, w_m\}$.

1: **for** $r = 0, 1, \cdots, R - 1$ **do**
2:      Set $\eta_i^{(r)} = \max\left\{\nu, \|v^{(r)} - w_i\|\right\}$ and $\beta_i^{(r)} = \alpha_i / \eta_i^{(r)}$ for $i = 1, \cdots, m$.
3:      Set $v^{(r+1)} = \left(\sum_{i=1}^m \beta_i^{(r)} w_i\right) / \left(\sum_{i=1}^m \beta_i^{(r)}\right)$.

Output: $v^{(r)}$.

---

where

$$\|z\|_{(\nu)} := \max_{u^\top u \leq 1} \left\{ u^\top z - \frac{\nu}{2} u^\top u \right\} + \frac{\nu}{2} = \begin{cases} \frac{1}{2\nu} \|z\|^2 + \frac{\nu}{2}, & \|z\| \leq \nu \\ \|z\|, & \|z\| > \nu \end{cases}. \tag{12}$$

In case $\nu = 0$, we define $g_0 \equiv g$. It is known [12] that $\|\cdot\|_{(\nu)}$ is $(1/\nu)$-smooth and that

$$0 \leq \|\cdot\|_{(\nu)} - \|\cdot\| \leq \nu/2 \tag{13}$$

Under Assumption 7, g_ν has a unique minimizer as well, denoted by $v_\nu^\star$. We call $v_\nu^\star$ as the ν-smoothed geometric median.

We let B denote the diameter of the convex hull of $\{w_1, \cdots, w_m\}$, i.e.,

$$B := \text{diam}(\text{conv}\{w_1, \cdots, w_m\}) = \max_{z, z' \in \text{conv}\{w_1, \cdots, w_m\}} \|z - z'\|. \tag{14}$$

We also assume that $\nu < B$, since for all $\nu \geq B$, the function g_ν is simply a quadratic for all $z \in$ conv$\{w_1, \cdots, w_m\}$.

C.2 Weiszfeld's Algorithm: Review

The Weiszfeld algorithm [85] performs the iterations

$$v^{(r+1)} = \begin{cases} \left(\sum_{i=1}^m \beta_i^{(r)} w_i\right) / \left(\sum_{i=1}^m \beta_i^{(r)}\right), & \text{if } v^{(r)} \notin \{w_1, \cdots, w_i\}, \\ w_i, & \text{if } v^{(r)} = w_i \text{ for some } k, \end{cases} \tag{15}$$

where $\beta_i^{(r)} = \alpha_i / \|v^{(r)} - w_i\|$. It was shown in [49, Thm. 3.4] that the sequence $\left(v^{(r)}\right)_{t=0}^\infty$ converges to the minimizer of g from (10), provided no iterate coincides with one of the w_i's. We modify Weiszfeld's algorithm to find the smoothed geometric median by considering

$$v^{(r+1)} = \frac{\sum_{i=1}^m \beta_i^{(r)} w_i}{\sum_{i=1}^m \beta_i^{(r)}}, \quad \text{where,} \quad \beta_i^{(r)} = \frac{\alpha_i}{\max\left\{\nu, \|v^{(r)} - w_i\|\right\}}. \tag{16}$$

This is also stated in Algorithm 5. Since each iteration of Weiszfeld's algorithm or its smoothed variant consists in taking a weighted average of the w_i's, the time complexity is $\mathcal{O}(md)$ floating point operations per iteration.

C.3 Derivation

We now derive Weiszfeld's algorithm with smoothing as as an alternating minimization algorithm or as an iterative minimization of a majorizing objective.

Surrogate Definition. Consider $\eta = (\eta_1, \cdots, \eta_m) \in \mathbb{R}^m$ and define $G : \mathbb{R}^d \times \mathbb{R}^m_{++} \to \mathbb{R}$ as

$$G(z, \eta) = \frac{1}{2} \sum_{i=1}^m \alpha_i \left(\frac{\|z - w_i\|^2}{\eta_i} + \eta_i \right). \tag{17}$$

Note firstly that G is jointly convex in z, η over its domain.

The first claim shows how to recover g and g_ν from G.

Claim 8. *Consider g, g_ν and G defined in Equations* (10), (11) *and* (17), *and fix $\nu > 0$. Then we have the following:*

$$g(z) = \inf_{\eta_1, \cdots, \eta_i > 0} G(z, \eta), \quad \text{and,} \tag{18}$$

$$g_\nu(z) = \min_{\eta_1, \cdots, \eta_i \geq \nu} G(z, \eta). \tag{19}$$

Proof. Define $G_i : \mathbb{R}^d \times \mathbb{R}_{++} \to \mathbb{R}$ by

$$G_i(z, \eta_i) := \frac{1}{2} \left(\frac{\|z - w_i\|^2}{\eta_i} + \eta_i \right),$$

so that $G(z, \eta) = \sum_{i=1}^m \alpha_i G_i(z, \eta_i)$.

Since $\eta_i > 0$, the arithmetic-geometric mean inequality implies that $G_i(z, \eta_i) \geq \|z - w_i\|$ for each i. When $\|z - w_i\| > 0$, the inequality above holds with equality when $\|z - w_i\|^2 / \eta_i = \eta_i$, or equivalently, $\eta_i = \|z - w_i\|$. On the other hand, when $\|z - w_i\| = 0$, let $\eta_i \to 0$ to conclude that

$$\inf_{\eta_i > 0} G_i(z, \eta_i) = \|z - w_i\|.$$

For the second part, we note that if $\|z - w_i\| \geq \nu$, then $\eta_i = \|z - w_i\| \geq \nu$ minimizes $G_i(z, \eta_i)$, so that $\min_{\eta_i \geq \nu} G_i(z, \eta_i) = \|z - w_i\|$. On the other hand, when $\|z - w_i\| < \nu$, we note that $G_i(z, \cdot)$ is minimized over $[\nu, \infty)$ at $\eta_i = \nu$, in which case we get $G_i(z, \eta) = \|z - w_i\|^2 / (2\nu) + \nu/2$. From (12), we conclude that

$$\min_{\eta_i \geq \nu} G_i(z, \eta_i) = \|z - w_i\|_{(\nu)}.$$

The proof is complete since $G(z, \eta) = \sum_{i=1}^m \alpha_i G_i(z, \eta_i)$. $\qquad\square$

Claim 8 now allows us to consider the following problem in lieu of minimizing g_ν from (11).

$$\min_{\substack{z \in \mathbb{R}^d, \\ \eta_1, \cdots, \eta_m \geq \nu}} G(z, \eta). \tag{20}$$

Alternating Minimization. Next, we consider an alternating minimization algorithm to minimize G in z, η. The classical technique of alternating minimization method, known also as the block-coordinate or block-decomposition method [see, e.g., 14], minimizes a function $f : X \times Y \to \mathbb{R}$ using the updates

$$x^{(r+1)} = \arg\min_{x \in X} f(x, y^{(r)}) \quad \text{and,} \quad y^{(r+1)} = \arg\min_{y \in Y} f(x^{(r+1)}, y).$$

Application of this method to Problem (20) yields the updates

$$\eta^{(r)} = \underset{\eta_1, \cdots, \eta_m \geq \nu}{\arg\min} \, G(v^{(r)}, \eta) = \left(\underset{\eta_i \geq \nu}{\arg\min} \left\{ \frac{\|v^{(r)} - w_i\|^2}{\eta_i} + \eta_i \right\} \right)_{i=1}^{m},$$

$$v^{(r+1)} = \underset{z \in \mathbb{R}^d}{\arg\min} \, G(z, \eta^{(r)}) = \underset{z \in \mathbb{R}^d}{\arg\min} \sum_{i=1}^{m} \frac{\alpha_i}{\eta_i^{(r)}} \|z - w_i\|^2 \,. \tag{21}$$

These updates can be written in closed form as

$$\eta_i^{(r)} = \max\{\nu, \|v^{(r)} - w_i\|\} \,,$$

$$v^{(r+1)} = \left(\sum_{i=1}^{m} \frac{\alpha_i}{\eta_i^{(r)}} w_i \right) \bigg/ \left(\sum_{i=1}^{m} \frac{\alpha_i}{\eta_i^{(r)}} \right) \,. \tag{22}$$

This gives the smoothed Weiszfeld algorithm, as pointed out by the following claim.

Claim 9. *For any fixed $\nu > 0$ and starting point $v^{(0)} \in \mathbb{R}^d$, the sequences $\left(v^{(r)}\right)$ produced by (16) and (22), and hence, (21) are identical.*

Proof. Follows from plugging in the expression from $\eta_i^{(r)}$ in the update for $v^{(r+1)}$ in (22). $\qquad\square$

Majorization-Minimization. We now instantiate the smoothed Weiszfeld algorithm as a majorization-minimization scheme. In particular, it is the iterative minimization of a first-order surrogate in the sense of [63, 64].

Define $g_\nu^{(r)} : \mathbb{R}^d \to \mathbb{R}$ as

$$g_\nu^{(r)}(z) := G(z, \eta^{(r)}) \,, \tag{23}$$

where $\eta^{(r)}$ is as defined in (21). The z-step of (21) simply sets $v^{(r+1)}$ to be the minimizer of $g_\nu^{(r)}$.

We note the following properties of $g_\nu^{(r)}$.

Claim 10. *For $g_\nu^{(r)}$ defined in (23), the following properties hold:*

$$g_\nu^{(r)}(z) \geq g_\nu(z) \,, \quad \text{for all } z \in \mathbb{R}^d \,, \tag{24}$$

$$g_\nu^{(r)}(v^{(r)}) = g_\nu(v^{(r)}) \,, \quad \text{and,} \tag{25}$$

$$\nabla g_\nu^{(r)}(v^{(r)}) = \nabla g_\nu(v^{(r)}) \,. \tag{26}$$

Moreover $g^{(r)}$ can also be written as

$$g_\nu^{(r)}(z) = g_\nu(v^{(r)}) + \nabla g_\nu(v^{(r)})^\top \left(z - v^{(r)} \right) + \frac{L^{(r)}}{2} \|z - v^{(r)}\|^2 \,, \tag{27}$$

where

$$L^{(r)} := \sum_{i=1}^{m} \frac{\alpha_i}{\eta_i^{(r)}} \,. \tag{28}$$

Proof. The first part follows because

$$g_\nu(z) = \min_{\eta_1,\cdots,\eta_m} G(z,\eta) \leq G(z,\eta^{(r)}) = g_\nu^{(r)}(z).$$

For Eq. (25), note that the inequality above is an equality at $v^{(r)}$ by the definition of $\eta^{(r)}$ from (21). To see (26), note that

$$\nabla g_\nu(z) = \sum_{i=1}^m \alpha_m \frac{z - w_i}{\max\{\nu, \|z - w_i\|\}}.$$

Then, by the definition of $\eta^{(r)}$ from (22), we get that

$$\nabla g_\nu(v^{(r)}) = \sum_{i=1}^m \frac{\alpha_m}{\eta_i^{(r)}} (v^{(r)} - w_i) = \nabla g_\nu^{(r)}(v^{(r)}).$$

The obtain the expansion (27), we write out the Taylor expansion of the quadratic $g^{(r)}(z)$ around $v^{(r)}$ to get

$$g_\nu^{(r)}(z) = g_\nu^{(r)}(v^{(r)}) + \nabla g_\nu^{(r)}(v^{(r)})^\top \left(z - v^{(r)}\right) + \frac{L^{(r)}}{2} \|z - v^{(r)}\|^2,$$

and complete the proof by plugging in (25) and (26). □

Gradient Descent. The next claim rewrites the smoothed Weiszfeld algorithm as gradient descent on g_ν.

Claim 11. *Equation* (16) *can also be written as*

$$v^{(r+1)} = v^{(r)} - \frac{1}{L^{(r)}} \nabla g_\nu(v^{(r)}), \tag{29}$$

where $L^{(r)}$ is as defined in (28).

Proof. Use $v^{(r+1)} = \arg\min_{z \in \mathbb{R}^d} g_\nu^{(r)}(z)$, where $g_\nu^{(r)}$ is written using (27). □

C.4 Properties of Iterates

The first claim reasons about the iterates $v^{(r)}, \eta^{(r)}$.

Claim 12. *Starting from any $v^{(0)} \in \mathrm{conv}\{w_1, \cdots, w_m\}$, the sequences $(\eta^{(r)})$ and $(v^{(r)})$ produced by Algorithm 5 satisfy*

- *$v^{(r)} \in \mathrm{conv}\{w_1, \cdots, w_m\}$ for all $t \geq 0$, and,*

- *$\nu \leq \eta_i^{(r)} \leq B$ for all $i = 1, \cdots, m$, and $t \geq 1$,*

where $B = \mathrm{diam}(\mathrm{conv}\{w_1, \cdots, w_m\})$. Furthermore, $L^{(r)}$ defined in (28) satisfies $1/B \leq L^{(r)} \leq 1/\nu$ for all $t \geq 0$.

Proof. The first part follows for $t \geq 1$ from the update (16), where Claim 9 shows the equivalence of (16) and (21). Then case of $t = 0$ is assumed. The second part follows from (22) and the first part. The bound on $L^{(r)}$ follows from the second part since $\sum_{i=1}^m \alpha_i = 1$. □

The next result shows that it is a descent algorithm. Note that the non-increasing nature of the sequence $\left(g_\nu(v^{(r)})\right)$ also follows from the majorization-minimization viewpoint [64]. Here, we show that this sequence is strictly decreasing. Recall that $v_\nu^\star$ is the unique minimizer of g_ν.

Lemma 13. *The sequence* $(v^{(r)})$ *produced by Algorithm 5 satisfies* $g_\nu(v^{(r+1)}) < g_\nu(v^{(r)})$ *unless* $v^{(r)} = v_\nu^\star$.

Proof. Let $\mathcal{E}_\nu = \{\eta \in \mathbb{R}^m : \eta_i \geq \nu \text{ for } k = 1, \cdots, m\}$. Starting with (19), we successively deduce,

$$
\begin{aligned}
g_\nu(v^{(r+1)}) &= \min_{\eta_1, \cdots, \eta_m \geq \nu} G(v^{(r+1)}, \nu) \\
&\leq G(v^{(r+1)}, \eta^{(r)}) \\
&= \min_{z \in \mathbb{R}^d} G(z, \eta^{(r)}) \\
&\leq G(v^{(r)}, \eta^{(r)}) \\
&= \min_{\eta_1, \cdots, \eta_m \geq \nu} G(v^{(r)}, \eta) \\
&= g_\nu(v^{(r)}).
\end{aligned}
$$

Here, we used the fact that $v^{(r+1)}$ minimizes $G(\cdot, \eta^{(r)})$ over $\mathbb{R}^d$ and that $\eta^{(r)}$ minimizes $G(v^{(r)}, \cdot)$ over $\mathcal{E}_\nu$.

Suppose now that $g_\nu(v^{(r+1)}) = g_\nu(v^{(r)})$. In this case, both the inequalities above hold with equality. Since $G(\cdot, \eta^{(r)})$ is $L^{(r)}$-strongly convex where $L^{(r)} \geq 1/B$ (cf. Claim 12), this implies that $v^{(r)} = \arg\min_{z \in \mathbb{R}^d} G(z, \eta^{(r)})$. By definition then, $\eta^{(r+1)} = \eta^{(r)}$ is the unique minimizer of $G(v^{(r)}, \cdot)$ over S, since $G(v^{(r)}, \cdot)$ is strictly convex. The associated first-order optimality conditions are the following:

$$
\nabla_z G(v^{(r)}, \eta^{(r)}) = 0, \quad \text{and,} \quad \nabla_\eta G(v^{(r)}, \eta^{(r)})^\top (\eta - \eta^{(r)}) \geq 0 \quad \forall \eta \in \mathcal{E}_\nu.
$$

Putting these together, we find that the pair $(v^{(r)}, \eta^{(r)})$ satisfies the first-order optimality conditions for G over the domain $\mathbb{R}^d \times \mathcal{E}_\nu$. Hence, $v^{(r)} = v_\nu^\star$. $\qquad\square$

The next lemma shows that $\|v^{(r)} - z^\star\|$ is non-increasing. This property was shown in [11, Corollary 5.1] for the case of Weiszfeld algorithm without smoothing.

Lemma 14. *The sequence* $(v^{(r)})$ *produced by Algorithm 5 satisfies for all* $t \geq 0$,

$$
\|v^{(r+1)} - v_\nu^\star\| \leq \|v^{(r)} - v_\nu^\star\|.
$$

Furthermore, if $g_\nu(v^{(r+1)}) \geq g_\nu(z^\star)$, *then it holds that*

$$
\|v^{(r+1)} - z^\star\| \leq \|v^{(r)} - z^\star\|.
$$

Proof. First note from Claim 11 that

$$
\nabla g_\nu(v^{(r)}) = L^{(r)}(v^{(r)} - v^{(r+1)}), \tag{30}
$$

where $L^{(r)}$ is defined in (28). Starting from the results of Claim 10, we observe for any z that,

$$
\begin{aligned}
g_\nu(v^{(r+1)}) &\overset{(24)}{\leq} g_\nu^{(r)}(v^{(r+1)}) \\
&\overset{(27)}{=} g_\nu(v^{(r)}) + \nabla g_\nu(v^{(r)})^\top \left(v^{(r+1)} - v^{(r)} \right) + \frac{L^{(r)}}{2} \|v^{(r+1)} - v^{(r)}\|^2 \\
&\overset{(*)}{\leq} g_\nu(z) + \nabla g_\nu(v^{(r)})^\top \left(v^{(r+1)} - z \right) + \frac{L^{(r)}}{2} \|v^{(r+1)} - v^{(r)}\|^2 \\
&\overset{(30)}{=} g_\nu(z) + L^{(r)} \left(v^{(r)} - v^{(r+1)} \right)^\top \left(v^{(r+1)} - z \right) + \frac{L^{(r)}}{2} \|v^{(r+1)} - v^{(r)}\|^2,
\end{aligned}
$$

7

where $(*)$ following from the convexity of g_ν as $g_\nu(z) \ge g_\nu(v^{(r)}) + \nabla g_\nu(v^{(r)})^\top (z - v^{(r)})$. Next, we use the Pythagorean identity: for any $a, b, c \in \mathbb{R}^d$, it holds that

$$\|b - a\|^2 + 2(b - a)^\top (a - c) = \|b - c\|^2 - \|a - c\|^2 \,.$$

With this, we get,

$$g_\nu(v^{(r+1)}) \le g_\nu(z) + \frac{L^{(r)}}{2} \left(\|v^{(r)} - z\|^2 - \|v^{(r+1)} - z\|^2 \right) \,.$$

Plugging in $z = v_\nu^\star$, the fact that $g_\nu(v^{(r+1)}) \ge g_\nu(z^\star)$ implies that $\|v^{(r+1)} - v_\nu^\star\|^2 \le \|v^{(r)} - v_\nu^\star\|^2$, since $L^{(r)} \ge 1/B$ is strictly positive. Likewise, for $z = z^\star$, the claim holds under the condition that $g_\nu(v^{(r+1)}) \ge g_\nu(z^\star)$. $\qquad\square$

C.5 Rate of Convergence

We are now ready to prove the global sublinear rate of convergence of Algorithm 5.

Theorem 15. *The iterate $v^{(R)}$ produced by Algorithm 5 with input $v^{(0)} \in \mathrm{conv}\{w_1, \cdots, w_m\}$ and $\nu > 0$ satisfies*

$$g_\nu(v^{(R)}) - g_\nu(z_\nu^\star) \le \frac{2\|v^{(0)} - z_\nu^\star\|^2}{\sum_{s=0}^{R-1} 1/L^{(s)}} \le \frac{2\|v^{(0)} - z_\nu^\star\|^2}{\widehat{\nu} R} \,,$$

where $L^{(s)} = \sum_{i=1}^m \alpha_i / \eta_i^{(s)}$ is defined in (28), and

$$\widehat{\nu} = \min_{s=0,\cdots,R-1} \min_{i \in [m]} \max\{\nu, \|v^{(s)} - w_i\|\} \ge \nu \,. \tag{31}$$

Furthermore, it holds that

$$g(v^{(R)}) - g(z^\star) \le \frac{2\|v^{(0)} - z^\star\|^2}{\sum_{s=0}^{R-1} 1/L^{(s)}} + \frac{\nu}{2} \le \frac{2\|v^{(0)} - z^\star\|^2}{\widehat{\nu} R} + \frac{\nu}{2} \,.$$

Proof. With the descent and contraction properties of Lemma 13 and Lemma 14 respectively, the proof now follows the classical proof technique of gradient descent [e.g., 71, Theorem 2.1.13]. Starting from the results of Claim 10, we observe for any z that,

$$g_\nu(v^{(r+1)}) \overset{(24)}{\le} g_\nu^{(r)}(v^{(r+1)})$$

$$\overset{(27)}{=} g_\nu(v^{(r)}) + \nabla g_\nu(v^{(r)})^\top \left(v^{(r+1)} - v^{(r)} \right) + \frac{L^{(r)}}{2} \|v^{(r+1)} - v^{(r)}\|^2$$

$$\overset{(29)}{=} g_\nu(v^{(r)}) - \frac{1}{2L^{(r)}} \|\nabla g_\nu(v^{(r)})\|^2 \,. \tag{32}$$

Convergence on g_ν. For ease of notation, we let $\widetilde{\Delta}_r := g_\nu(v^{(r)}) - g_\nu(v_\nu^\star)$. We assume now that $\widetilde{\Delta}_{r+1}$ is nonzero, and hence, so is $\widetilde{\Delta}_r$ (Lemma 13). If $\widetilde{\Delta}_{r+1}$ were zero, then the theorem would hold trivially at $t + 1$.

Now, from convexity of g_ν and the Cauchy-Schwartz inequality, we get that

$$\widetilde{\Delta}_r \le \nabla g_\nu(v^{(r)})^\top \left(v^{(r)} - z_\nu^\star \right) \le \|\nabla g_\nu(v^{(r)})\| \|v^{(r)} - z_\nu^\star\| \,.$$

Plugging this in, we get,

$$\widetilde{\Delta}_{r+1} - \widetilde{\Delta}_r \le -\frac{1}{2L^{(r)}}\frac{\widetilde{\Delta}_r^2}{\|v^{(r)} - z_\nu^\star\|^2}$$

$$\le -\frac{1}{2L^{(r)}}\frac{\widetilde{\Delta}_r^2}{\|v^{(0)} - z_\nu^\star\|^2},$$

where we invoked Lemma 14.

Now, we divide by $\widetilde{\Delta}_r\widetilde{\Delta}_{r+1}$, which is nonzero by assumption, and use $\widetilde{\Delta}_r/\widetilde{\Delta}_{r+1} \ge 1$ (Lemma 13) to get

$$\frac{1}{\widetilde{\Delta}_r} - \frac{1}{\widetilde{\Delta}_{r+1}} \le -\frac{1}{2L^{(r)}}\left(\frac{\widetilde{\Delta}_r}{\widetilde{\Delta}_{r+1}}\right)\frac{1}{\|v^{(0)} - z_\nu^\star\|^2}$$

$$\le -\frac{1}{2L^{(r)}\|v^{(0)} - z_\nu^\star\|^2}.$$

Telescoping, we get,

$$\frac{1}{\widetilde{\Delta}_r} \ge \frac{1}{\widetilde{\Delta}_r} - \frac{1}{\widetilde{\Delta}_0} \ge \left(\sum_{s=0}^{r-1}\frac{1}{L^{(s)}}\right)\frac{1}{2\|v^{(0)} - z_\nu^\star\|^2}.$$

This proves the first inequality to be proved. The second inequality follows from the definition in Eq. (28) since $\sum_{i=1}^m \alpha_i = 1$.

Convergence on g. The proof follows along the same ideas as the previous proof. Define $\Delta_r := g_\nu(v^{(r)}) - g_\nu(z^\star)$. Suppose $\Delta_r > 0$. Then, we proceed as previously for any $s < t$ to note by convexity and Cauchy-Schwartz inequality that

$$\Delta_s \le \|\nabla g_\nu(v^{(s)})\|\|v^{(s)} - z^\star\|.$$

Again, plugging this into (32), using that $\Delta_s/\Delta_{s+1} \ge 1$ and invoking Lemma 14 gives (since $\Delta_s > 0$)

$$\frac{1}{\Delta_s} - \frac{1}{\Delta_{s+1}} \le -\frac{1}{2L^{(s)}\|v^{(0)} - z^\star\|^2}.$$

Telescoping and taking the reciprocal gives

$$g_\nu(v^{(R)}) - g_\nu(z^\star) = \Delta_r \le \frac{2\|v^{(0)} - z^\star\|^2}{\sum_{s=0}^{R-1}1/L^{(s)}}.$$

Using (13) completes the proof for the case that $\Delta_r > 0$. Note that if $\Delta_r \le 0$, it holds that $\Delta_{t'} \le 0$ for all $t' > t$. In this case, $g_\nu(v^{(r)}) - g_\nu(z^\star) \le 0$. Again, (13) implies that $g(v^{(r)}) - g(z^\star) \le \nu/2$, which is trivially upper bounded by the quantity stated in the theorem statement. This completes the proof. $\square$

Faster Rate of Convergence. We now make an additional assumption:

Assumption 16. *The geometric median $z^\star$ does not coincide with any of $w_1, \cdots, w_m$. In other words,*

$$\widetilde{\nu} := \min_{i=1,\cdots,m}\|z^\star - w_i\| > 0.\tag{33}$$

Remark 17. *[11, Lemma 8.1] show a lower bound on $\widetilde{\nu}$ in terms of $\alpha_1, \cdots, \alpha_m$ and $w_1, \cdots, w_m$.*

Now, we analyze the condition under which the $z^\star = v_\nu^\star$.

Lemma 18. *Under Assumption 16, we have that $z^\star = v_\nu^\star$ for all $\nu \le \widetilde{\nu}$, where $\widetilde{\nu}$ is defined in* (33).

Proof. By the definition of the smooth norm in (12), we observe that $\|z^\star - w_i\|_{(\nu)} = \|z^\star - w_i\|$ for all $\nu \le \widetilde{\nu}$, and hence, $g_\nu(z^\star) = g(z^\star)$. For any $z \in \mathbb{R}^d$, we have,

$$g_\nu(z) \overset{(13)}{\ge} g(z) \ge g(z^\star) = g_\nu(z^\star),$$

or that $z^\star = v_\nu^\star$. $\qquad\square$

In this case, we get a better rate on the non-smooth objective g.

Corollary 19. *Consider the setting of Theorem 15 where Assumption 16 holds and $\nu \le \widetilde{\nu}$. Then, the iterate $v^{(R)}$ produced by Algorithm 5 satisfies,*

$$g(v^{(r)}) - g(z^\star) \le \frac{2\|v^{(0)} - z^\star\|^2}{\widehat{\nu}R},$$

where $\widehat{\nu}$ is defined in Eq. (31).

Proof. This follows from Theorem 15's bound on $g_\nu(v^{(R)}) - g_\nu(v_\nu^\star)$ with the observations that $g(v^{(R)}) \overset{(13)}{\le} g_\nu(v^{(R)})$ and $g(z^\star) = g_\nu(z^\star)$ (see the proof of Lemma 18). $\qquad\square$

The previous corollary obtains the same rate as [11, Theorem 8.2], up to constants upon using the bound on $\widetilde{\nu}$ given by [11, Lemma 8.1].

We also get as a corollary a bound on the performance of Weiszfeld's original algorithm without smoothing, although it could be numerically unstable in practice. This bound depends on the actual iterates, so it is not informative about the performance of the algorithm a priori.

Corollary 20. *Consider the setting of Theorem 15. Under Assumption 16, suppose the sequence $(v^{(r)})$ produced by Weiszfeld's algorithm in Eq.* (15) *satisfies $\|v^{(r)} - w_i\| > 0$ for all r and i, then it also satisfies*

$$g(v^{(R)}) - g(z^\star) \le \frac{2\|v^{(0)} - z^\star\|^2}{\nu^{(R)}R}.$$

where $\nu^{(r)}$ is given by

$$\nu^{(r)} = \min\left\{\widetilde{\nu}, \min_{s=0,\cdots,r}\min_{i\in[m]}\|v^{(s)} - w_i\|\right\}.$$

Proof. Under these conditions, note that the sequence $(v^{(s)})_{s=0}^t$ produced by the Weiszfeld algorithm without smoothing coincides with the sequence $(v_{\nu^{(r)}}^{(s)})_{s=0}^t$ produced by the smoothed Weiszfeld algorithm at level $\nu = \nu^{(r)}$. Now apply Corollary 19. $\qquad\square$

C.6 Comparison to Previous Work

We compare the results proved in the preceding section to prior work on the subject.

Comparison to [11]. The authors present multiple different variants of the Weiszfeld algorithm. For a particular choice of initialization, they can guarantee that a rate of the order of $1/\widetilde{\nu}R$. It is not clear how this choice of initialization can be implemented using a secure average oracle since, if at all. This is because it requires the computation of all pairwise distances $\|w_i - w_{i'}\|$. Moreover, a naive implementation of their algorithm could be numerically unstable since it would involve division by small numbers. Guarding against division by small numbers would lead to the smoothed variant considered here. Note that our algorithmic design choices are driven by the federated learning setting.

Comparison to [10]. The author studies general alternating minimization algorithms, including the Weiszfeld algorithm as a special case, with a different smoothing than the one considered here. While their algorithm does not suffer from numerical issues arising from division by small numbers, it always suffers a bias from smoothing. On the other hand, the smoothing considered here is more natural in that it reduces to Weiszfeld's original algorithm when $\|v^{(r)} - w_i\| > \nu$, i.e., when we are not at a risk of dividing by small numbers. Furthermore, the bound in Theorem 15 exhibits a better dependence on the initialization $v^{(0)}$.

D   Numerical Simulations: Full Details

The section contains a full description of the experimental setup as well as additional results.

We start with the dataset and task description in Appendix D.1, hyperparameter choices in Appendix D.2, and evaluation methodology in Appendix D.3. We provide some extra numerical results in Appendix D.5.

D.1   Datasets and Task Description

We experiment with three tasks, (1) handwritten-letter recognition, (2) character-level language modeling, and, (3) sentiment analysis. As discussed in Section 3.1, we take the weight $\alpha_i \propto N_i$, which is the number of data points available on device i.

D.1.1   Handwritten-Letter Recognition

The first dataset is the EMNIST dataset [26] for handwritten letter recognition.

Data. Each inpt x is a gray-scale image resized to 28×28. Each output y is categorical variable which takes 62 different values, one per class of letter (0-9, a-z, A-Z).

Formulation. The task of handwritten letter recognition is cast as a multi-class classification problem with 62 classes.

Distribution of Data. The handwritten characters in the images are annotated by the writer of the character as well. We use a non-i.i.d. split of the data grouped by a writer of a given image. We discard devices with less than 100 total input-output pairs (both train and test), leaving a total of 3461 devices. Of these, we sample 1000 devices to use for our simulations, corresponding to about 30% of the data. This selection held constant throughout the simulations. The number of training examples across these devices summarized in the following statistics: median 160, mean 202, standard deviation 77, maximum 418 and minimum 92. This preprocessing was performed using LEAF [19].

Models. For the model φ, we consider two options: a linear model and a convolutional neural network.
- Linear Model: The linear model maintains parameters $w_1, \cdots, w_{62} \in \mathbb{R}^{28 \times 28}$. For a given image x, class l is assigned score $\langle w_l, x \rangle$, which is then converted to a probability using a softmax operation as $p_l = \exp(\langle w_l, x \rangle) / \sum_{l'} \exp(\langle w_{l'}, x \rangle)$. For a new input image x, the prediction is made as $\arg\max_l \langle w_l, x \rangle$.
- Convolutional Neural Network (ConvNet): The ConvNet [54] we consider contains two convolutional layers with max-pooling, followed by a fully connected hidden layer, and another fully connected (F.C.) layer with 62 outputs. When given an input image x, the output of this network is assigned as the scores of each of the classes. Probabilities are assigned similar to the linear model with a softmax operation on the

11

scores. The schema of network is given below:

$$\begin{array}{c}
\text{Input} \\
28 \times 28
\end{array} \longrightarrow
\begin{array}{c}
\text{Conv2D} \\
\text{filters} = 32 \\
\text{kernel} = 5 \times 5
\end{array} \longrightarrow \text{ReLU} \longrightarrow
\begin{array}{c}
\text{Max Pool} \\
\text{kernel} = 2 \times 2 \\
\text{stride} = 2
\end{array} \longrightarrow
\begin{array}{c}
\text{Conv2D} \\
\text{filters} = 64 \\
\text{kernel} = 5 \times 5
\end{array} \longrightarrow$$

$$\text{ReLU} \longrightarrow
\begin{array}{c}
\text{Max Pool} \\
\text{kernel} = 2 \times 2 \\
\text{stride} = 2
\end{array} \longrightarrow
\begin{array}{c}
\text{F.C.} \\
\text{units} = 2048
\end{array} \longrightarrow \text{ReLU} \longrightarrow
\begin{array}{c}
\text{F.C.} \\
\text{units} = 62
\end{array} \longrightarrow \text{score}$$

Loss Function. We use the multinomial logistic loss $\ell(y, p) = -\log p_y$, for probabilities $p = (p_1, \cdots, p_{62})$ and $y \in \{1, \cdots, 62\}$. In the linear model case, it is equivalent to the classical softmax regression.

Evaluation Metric. The model is evaluated based on the classification accuracy on the test set.

D.1.2 Character-Level Language Modeling

The second task is to learn a character-level language model over the Complete Works of Shakespeare [78]. The goal is to read a few characters and predict the next character which appears.

Data. The dataset consists of text from the Complete Works of William Shakespeare as raw text.

Formulation. We formulate the task as a multi-class classification problem with 53 classes (a-z, A-Z, other) as follows. At each point, we consider the previous $H = 20$ characters, and build $x \in \{0, 1\}^{H \times 53}$ as a one-hot encoding of these H characters. The goal is then try to predict the next character, which can belong to 53 classes. In this manner, a text with l total characters gives l input-output pairs.

Distribution of Data. We use a non-i.i.d. split of the data. Each role in a given play (e.g., Brutus from The Tragedy of Julius Caesar) is assigned as a separate device. All devices with less than 100 total examples are discarded, leaving 628 devices. The training set is assigned a random 90% of the input-output pairs, and the other rest are held out for testing. This distribution of training examples is extremely skewed, with the following statistics: median 1170, mean 3579, standard deviation 6367, maximum 70600 and minimum 90. This preprocessing was performed using LEAF [19].

Models. We use a long-short term memory model (LSTM) [38] with 128 hidden units for this purpose. This is followed by a fully connected layer with 53 outputs, the output of which is used as the score for each character. As previously, probabilities are obtained using the softmax operation.

Loss Function. We use the multinomial logistic loss.

Evaluation Metric. The model is evaluated based on the accuracy of next-character prediction on the test set.

D.1.3 Sentiment Analysis

The third task is analyze the sentiment of tweets as positive or negative.

Data. Sent140 [36] is a text dataset of 1,600,498 tweets produced by 660,120 Twitter accounts. Each tweet is represented by a character string with emojis redacted. Each tweet is labeled with a binary sentiment reaction (i.e., positive or negative), which is inferred based on the emojis in the original tweet.

Formulation. The task is a binary classification problem, with the output being a positive or negative sentiment, while the input is the raw text of the tweet.

Distribution of Data. We use a non-i.i.d. split of the data. Each client device represents a Twitter user and contains tweets from this user. We discarded all clients containing less that 50 tweets, leaving only 877 clients. The training set is assigned a random 80% of the input-output pairs, and the other rest are held out for testing. This distribution of training examples across client devices is skewed, with the following statistics: median 55, mean 65.3, standard deviation 32.4, maximum 439 and minimum 40. This preprocessing was performed using LEAF [19].

Models. We use a linear model $\varphi(x; w) = w^\top \phi(x)$, where the feature representation $\phi(x) \in \mathbb{R}^{50}$ of text x is obtained as the average of the GloVe embeddings [74] $G(\cdot)$ of each word in the tweet, i.e.,

$$\phi(x) = \frac{1}{|x|} \sum_{i=1}^{|x|} G(x_i) \,.$$

Loss Function. We use the binary logistic loss.

Evaluation Metric. We use the binary classification accuracy.

D.2 Methods, Hyperparameters and Variants

We first describe the corruption model, followed by various methods tested.

D.2.1 Corruption Model

Since the goal of this work to test the robustness of federated learning models in the setting of high corruption, we artificially corrupt updates while controlling the level of corruption. We use the following corruption models.

Data Corruption. This is an example of static data poisoning. The model training procedure is not modified, but the data fed into the model is modified. In particular, we take a modification $\tilde{D}_i$ of the local dataset D_i of client i and run the training algorithm on this different dataset. The exact nature of the modification depends on the dataset:
- EMNIST: We take the negative of the image x. Mathematically, $\tilde{D}_i(x, y) = D_i(1 - x, y)$, assuming the pixels of x are normalized to lie in $[0, 1]$. The labels are left unmodified.
- Shakespeare: We reverse the original text. Mathematically, $\tilde{D}_i(c_1 \cdots c_{20}, c_{21}) = D_i(c_{21} \cdots c_2, c_1)$ This is illustrated in Fig. 7. The labels are left unmodified.
- Sent140: We flip the label, i.e., $\tilde{D}_i(x, y) = D_i(x, -y)$. The text in the tweet remains unchanged.

Text: the geometric **_m_**edian's robustness

x, y :   geometric   **_m_**

$\widetilde{x}, \widetilde{y}$:   or s'naide   **_m_**

Figure 7: Illustration of the data corruption introduced in the Shakespeare dataset. The first line denotes the original text. The second line shows the effective x when predicting the "m" of the word "median". The second line shows the corresponding $\widetilde{x}$ after the introduction of the corruption. Note that $\widetilde{x}$ is the string "edian's ro" reversed.

Gaussian corruption. This is an example of update poisoning. The data is not modified here but the update of a client device is directly replaced by a Gaussian random variable, with standard deviation σ equal to the standard deviation of the original update across its components. Note that we corrupt the *update* to the model parameters transmitted by the device, which is typically much smaller in norm than the model parameters themselves.

Omniscient corruption. This is an example of update poisoning. The data is not modified here but the parameters of a device are directly modified. In particular, $w_i^{(t+1)}$ for $i \in \mathcal{C}$ is set to be

$$w_i^{(t+1)} = -\frac{1}{\sum_{j \in S_t \cap \mathcal{C}} \alpha_j} \left(2 \sum_{j \in S_t \backslash \mathcal{C}} \alpha_j w_{j,\tau}^{(t)} + \sum_{j \in S_t \cap \mathcal{C}} \alpha_j w_{j,\tau}^{(t)} \right),$$

such that

$$\sum_{i \in S_t} \alpha_i w_i^{(t+1)} = -\sum_{i \in S_t} \alpha_i w_{i,\tau}^{(t)}.$$

In other words, the weighted arithmetic mean of the model parameter is set to be the negative of what it would have other been without the corruption. This corruption model requires full knowledge of the data and server state, and is adversarial in nature.

Implementation details. Given a corruption level ρ, the set of devices which return corrupted updates are selected as follows:
- Start with $\mathcal{C} = \varnothing$.
- Sample device i uniformly without replacement and add to $\mathcal{C}$. Stop when $\sum_{i \in C} \alpha_i$ just exceeds ρ.

D.2.2   Methods

We compare the following algorithms:
- the FedAvg algorithm [66],
- the RFA algorithm proposed here in Algorithm 1,
- the minibatch stochastic gradient descent (SGD) algorithm.

D.2.3   Hyperparameters

The hyperparameters for each of these algorithms are detailed below.

FedAvg. The FedAvg algorithm requires the following hyperparameters.
- Devices per round m: We use 100 for EMNIST and 50 for both the Shakespeare and Sent140 datasets.
- Batch Size and Number of Local Epochs: Instead of running τ local updates, we run for n_e local epochs following [66] with a batch size of b. For the EMNIST dataset, we use $b = 50, n_e = 5$, and for Shakespeare and Sent140, we use $b = 10, n_e = 1$.
- Learning Rate (γ_t): We use a learning a learning rate scheme $\gamma_t = \gamma_0 C^{\lfloor t/t_0 \rfloor}$, where γ_0 and C were tuned using grid search on validation set (20% held out from the training set) for a fixed time horizon on the uncorrupted data. The values which gave the highest validation accuracy were used *for all settings* - both corrupted and uncorrupted. The time horizon used was 2000 iterations for the EMNIST linear model, 1000 iterations for the EMNIST ConvNet 200 iterations for Shakespeare LSTM.
- Initial Iterate $w^{(0)}$: Each element of $w^{(0)}$ is initialized to a uniform random variable whose range is determined according to TensorFlow's "glorot_uniform_initializer".

RFA. RFA's hyperparameters, in addition to those of FedAvg, are:
- Algorithm: We use the smoothed Weiszfeld algorithm, as discussed in Sec. 4.
- Smoothing parameter ν: Based on the interpretation that ν guards against division by small numbers, we simply use $\nu = 10^{-6}$ throughout.
- Robust Aggregation Stopping Criterion: The concerns the stopping criterion used to terminate the smoothed Weiszfeld algorithm. We use two criteria: an iteration budget and a relative improvement condition - we terminate if a given iteration budget has been extinguished, or if the relative improvement in objective value $|g_\nu(v^{(r)}) - g_\nu(v^{(r+1)})|/g_\nu(v^{(r)}) \leq 10^{-6}$ is small.

D.3 Evaluation Methodology and Other Details

We specify here the quantities appearing on the x and y axes on the plots, as well as other details.

x **Axis.** As mentioned in Section 3, the goal of federated learning is to learn the model with as few rounds of communication as possible. Therefore, we evaluate various methods against the number of rounds of communication, which we measure via the number of calls to a secure average oracle.

Note that FedAvg and SGD require one call to the secure average oracle per outer iteration, while RFA could require several. Hence, we also evaluate performance against the number of outer iterations.

y **Axis.** We are primarily interested in the test accuracy, which measures the performance on unseen data. We also plot the function value F, which is the quantity our optimization algorithm aims to minimize. We call this the train loss.

Evaluation with Data Corruption. In simulations with data corruption, while the training is performed on corrupted data, we evaluate train and test progress using the corruption-free data.

Software. We use the package LEAF [19] to simulate the federated learning setting. The models used are implemented in TensorFlow.

Hardware. Each simulation was run in a simulation as a single process. The EMNIST linear model simulations were run on two workstations with 126GB of memory, with one equipped with Intel i9 processor running at 2.80GHz, and the other with Intel Xeon processors running at 2.40GHz. Simulations involving neural networks were run either on a 1080Ti or a Titan Xp GPU.
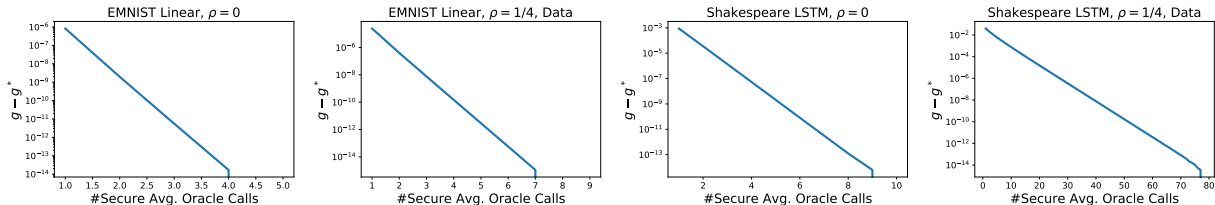
(a) Convergence of the smoothed Weiszfeld algorithm and for robust aggregation.
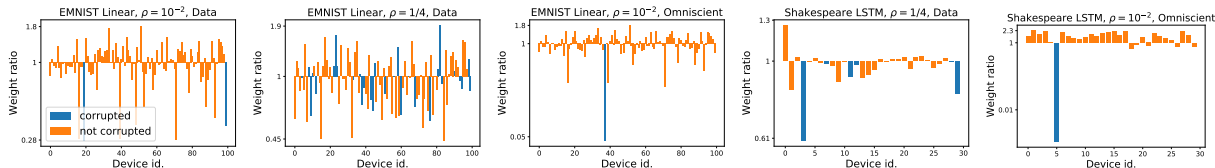
(b) Visualization of the re-weighting of points in the robust aggregate.

Figure 8: Performance of robust aggregation algorithms.

Random runs. Each simulation is repeated 5 times with different random seeds, and the solid lines in the plots here represents the mean over these runs, while the shaded areas show the maximum and minimum values obtained in these runs.

D.4 Simulation Results: Convergence of The Smoothed Weiszfeld Algorithm

For each of these models, we freeze FedAvg at a certain iteration and experiment with different robust aggregation algorithms.

We find that the smoothed Weiszfeld algorithm enjoys a fast convergence behavior, converging exactly to the smoothed geometric median in a few passes. In fact, the smoothed Weiszfeld algorithm displays (local) linear convergence, as evidenced by the straight line in log scale. Further, we also maintain a strict iteration budget of 3 iterations. This choice is also justified in hindsight by the results of Figure 10.

Next, we visualize the weights assigned by the geometric median to the corrupted updates. Note that the smoothed geometric median $w_1, \cdots, w_m$ is some convex combination $\sum_{i=1}^m \beta_i w_i$. This weight β_i of w_i is a measure of the influence of w_i on the aggregate. We plot in Figure 8b the ratio β_i/α_i for each device i, where α_i is its weight in the arithmetic mean and β_i is obtained by running the smoothed Weiszfeld algorithm to convergence. We expect this ratio to be smaller for worse corruptions and ideally zero for obvious corruptions. We find that the smoothed geometric median does indeed assign lower weights to the corruptions, while only accessing the points via a secure average oracle.

D.5 Additional Simulation Results

Effect of non-identical data distributions. Here, we plot the analogue of Figure 2 for the Sent140 dataset with data corruption in the setting where the dataset was split in an i.i.d. manner across devices. Recall that we had a small gap of 0.3% between the performance of RFA and FedAvg in the setting of no corruption. Consistent with the theory, this gap completely vanishes in the i.i.d. case, as shown in Figure 9.

Effect of iteration budget of smoothed Weiszfeld. We study the effect of the iteration budget of the smoothed Weiszfeld algorithm in RFA. in Figure 10. We observe that a low communication budget is faster in the regime of low corruption, while more iterations work better in the high corruption regime. We used a budget of 3 calls to the secure average oracle throughout to trade-off between these two scenarios.
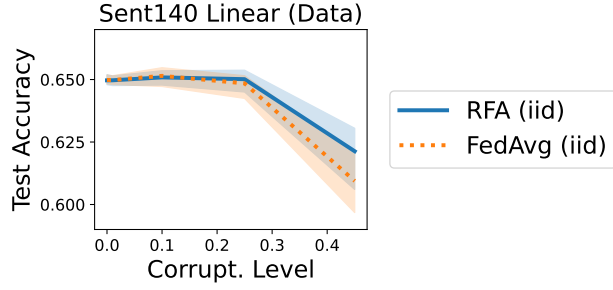
16

Figure 9: Robustness of RFA and FedAvg for an i.i.d. data split on Sent140 with data corruption.
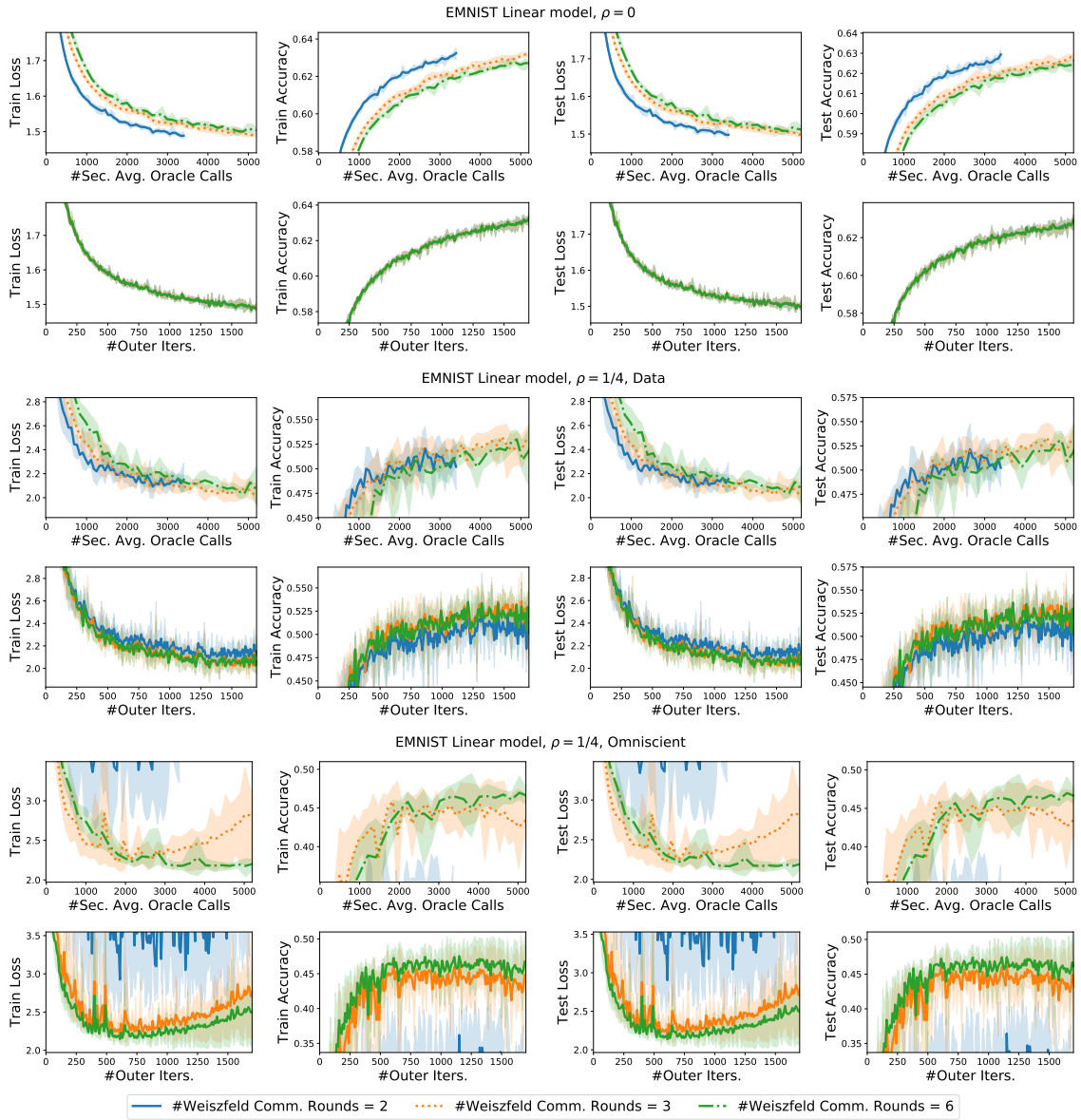

Figure 10: Hyperparameter study, effect of the maximum number of the communication budget on the smoothed Weiszfeld algorithm in RFA on the EMNIST dataset with a linear model.
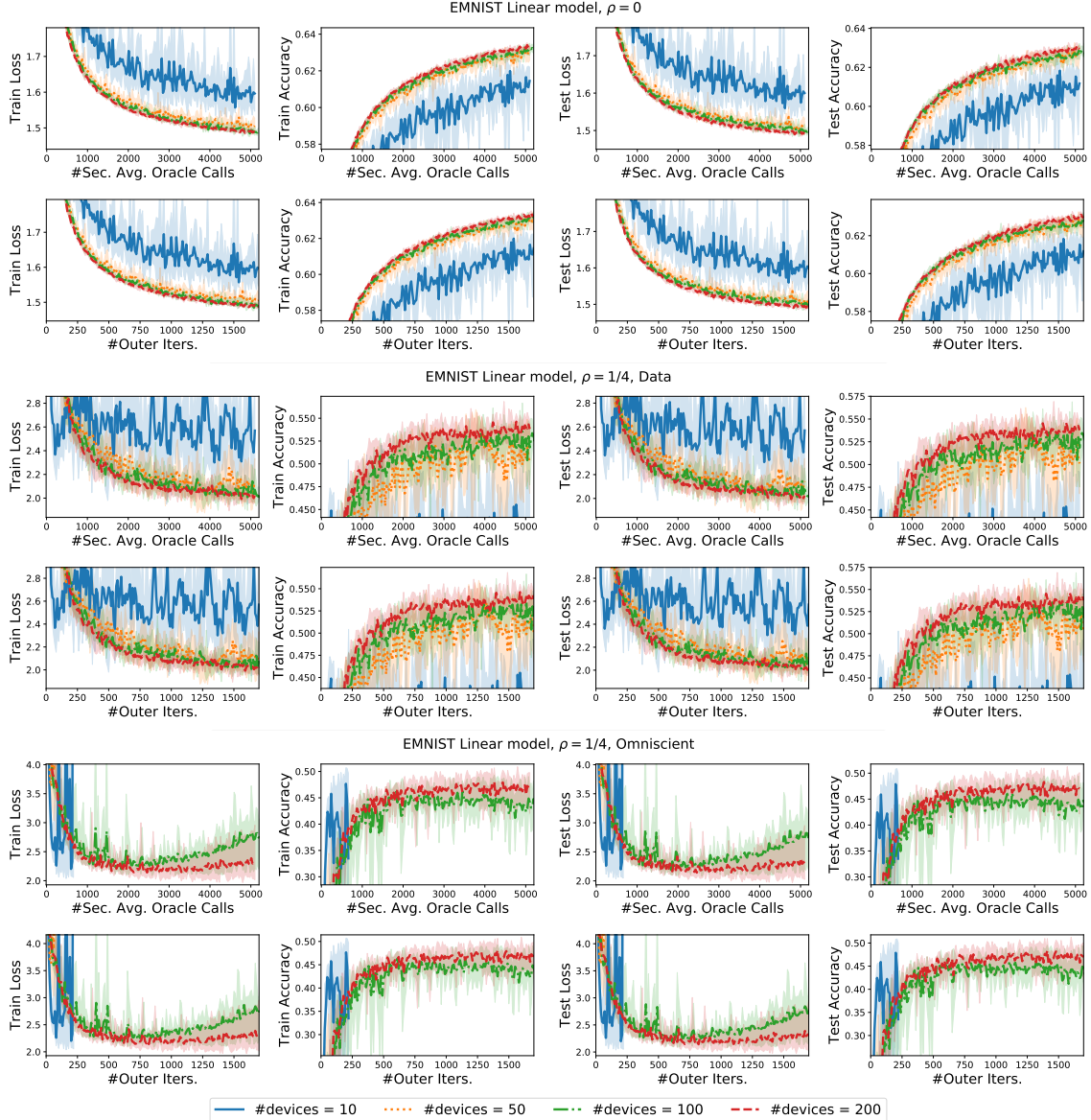
Figure 11: Hyperparameter study, effect of the number of selected client devices per round in RFA on the EMNIST dataset with a linear model.

Effect of number of devices per iteration round. Figure 11 plots the performance of RFA against the number m of devices chosen per round. We observe the following: in the regime of low corruption, good performance is achieved by selecting 50 devices per round (5%), where as 10 devices per round (1%) is not enough. On the other hand, in high corruption regimes, we see the benefit of choosing more devices per round, as a few runs with 10 or 50 devices per round with omniscient corruption at 25% diverged. This is consistent with Theorem 4, which requires the number of devices per round to increase with the level of corruption (cf. Eq. (9)).

Effect of local computation. Figure 12 plots the performance of FedAvg and RFA versus the amount of local computation. We see that the performance is always within one standard deviation of each other irrespective of the amount of local computation. However, we also note that RFA with a single local epoch is
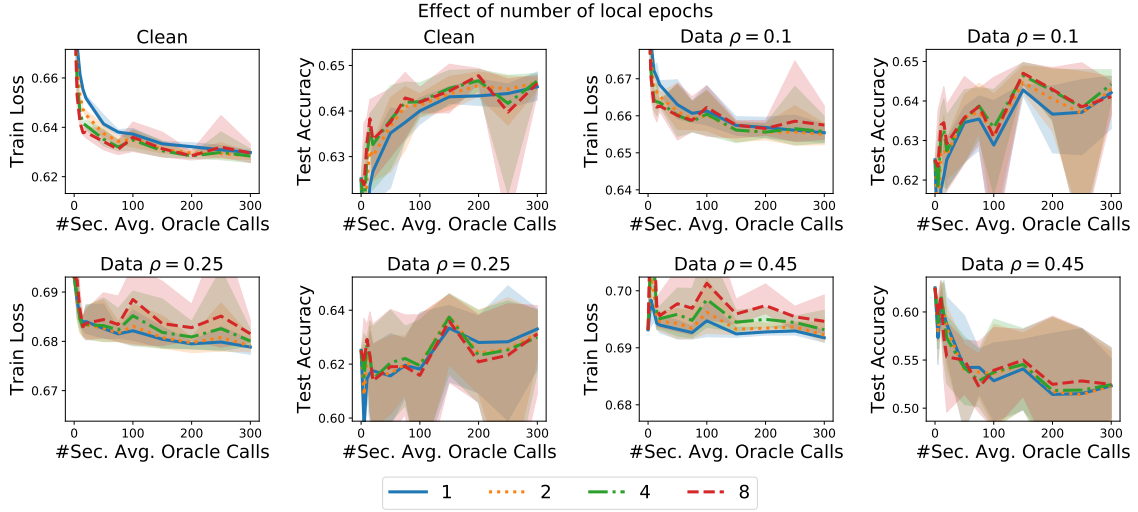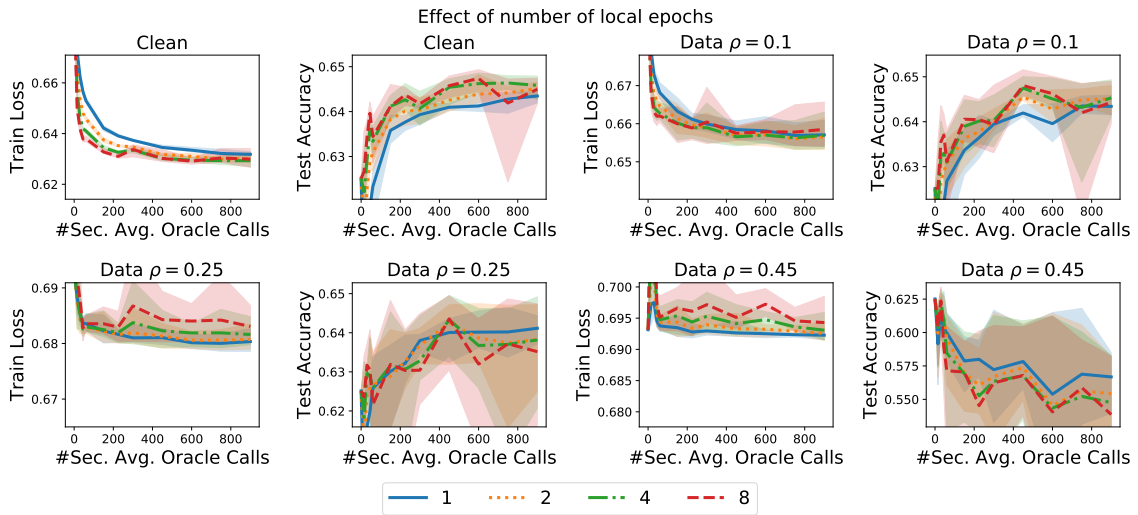
Figure 12: Effect of the number of epochs on FedAvg and RFA for the Sent140 dataset in the presence of data corruption.

obtains a slightly lower test accuracy in the no-corruption regime than using more local computation.